Three Subdivisions of the Auditory Midbrain in Chicks (*Gallus gallus*) Identified by Their Afferent and Commissural Projections

Yuan Wang[1,2]* and Harvey J. Karten[1]

[1]Department of Neurosciences, University of California at San Diego, La Jolla, California 92093-0608

[2]Department of Otolaryngology and Virginia Merrill Bloedel Hearing Research Center, University of Washington, Seattle, Washington 98195

ABSTRACT

The auditory midbrain is a site of convergence of multiple auditory channels from the brainstem. In birds, two separate ascending channels have been identified, through which time and intensity information is sent to the nucleus mesencephalicus lateralis, pars dorsalis (MLd), the homologue of the central nucleus of the mammalian inferior colliculus. Using in vivo anterograde and retrograde tracing techniques, the current study provides two lines of anatomical evidence supporting the presence of a third ascending channel to the chick MLd. First, three non-overlapping zones of the MLd receive inputs from three distinct cell groups in the caudodorsal brainstem. The projections from the nucleus angularis (NA) and nucleus laminaris (NL) are predominantly contralateral and may correspond to the time and intensity channels. A rostromedial portion of the MLd receives bilateral projections mainly from the *regio intermedius*, an interposed region of cells lying at a caudal level between the NL and NA, as well as scattered neurons embedded in the 8th nerve tract, and probably a very ventral region of the NA. Second, the bilateral zones of the MLd on two sides of the brain are reciprocally connected and do not interact with other zones of the MLd via commissural connections. In contrast, the NL-recipient zone projects contralaterally upon the NA-recipient zone. The structural separation of the third pathway from the NA and NL projections suggests a third information-processing channel, in parallel with the time and intensity channels. Neurons in the third channel appear to process very low frequency information including infrasound, probably utilizing different mechanisms than that underlying higher frequency processing. J. Comp. Neurol. 518:1199–1219, 2010. © 2009 Wiley-Liss, Inc.

INDEXING TERMS: cochlear nuclei; MLd, inferior colliculus; parallel organization; infrasound

In birds, ascending axons of the inner ear mainly terminate in two major auditory cell groups, the nucleus magnocellularis (NM) and the nucleus angularis (NA), as well as a number of vestibular nuclei in the brainstem (Holmes, 1903; Boord and Rasmussen, 1963; Parks and Rubel, 1978). In addition, fibers from the inner ear also terminate in less well circumscribed areas adjacent to, and between these nuclei (Boord and Rasmussen, 1963; Boord and Karten, 1974; Parks and Rubel, 1978; Kaiser and Manley, 1996). These nuclei contribute in differing manner and degree to ascending projections upon the nucleus mesencephalicus lateralis, pars dorsalis (MLd), the homologue of the central nucleus of the mammalian inferior colliculus. Convergence of these ascending projections within the MLd, as well as their interactions with the commissural projection from the contralateral MLd, is critical for the computation of sound localization (for review, see Knudsen, 1987; Klump, 2000) and the encoding of a wide range of complex sounds (Woolley and Casseday, 2004, 2005; Woolley et al., 2006).

The organization of the afferent and commissural projections to the avian MLd has mainly been studied in barn owls, a highly specialized species with well-developed

sound localization. In barn owls, the MLd receives intensity and time information through two separate ascending channels. The intensity channel arises from the contralateral NA, and the time channel from the contralateral nucleus laminaris (NL), which receives bilateral inputs from the NM (Sullivan and Konishi, 1984; Takahashi et al., 1984; Konishi et al., 1985; Takahashi and Konishi, 1986). Both channels contain monosynaptic and polysynaptic pathways, the latter via cell groups embedded in the lemniscus lateralis and the superior olive (Takahashi and Konishi, 1988a,b). Within the MLd, the NA and NL terminate in two non-overlapping zones that are biochemically distinct from each other (Takahashi et al., 1987; Takahashi and Konishi, 1988a; Adolphs, 1993; Wagner et al., 2003). This differential distribution is associated with the organization of the commissural connection between two MLds. The NL-recipient zone of the MLd projects in a restricted manner upon the lateral portion of the NA-recipient zone on the other side of the brain (Takahashi et al., 1989). This projection integrates time and intensity information and contributes to the computation of the spatial location of auditory stimuli (Takahashi et al., 1989).

Data from two more commonly studied avian species, chickens and pigeons, show similarities in the general pattern of two separate pathways from the NA and NL upon the MLd (Leibler, 1975; Conlee and Parks, 1986; Wild, 1995). However, notable discrepancies across species in the organization of the MLd and its afferent and commissural projections have been reported. One of the most distinct variations is a bilateral projection upon the MLd in chickens from the regions adjacent to, as well as partially embedded within, the NM, NL, and NA (Conlee and Parks, 1986). The separation of this bilateral projection from those arising from the contralateral NA and NL has not been adequately clarified. In addition, the NL-recipient zone of the MLd in pigeons is reported to be reciprocally connected (Leibler, 1975), in contrast to the commissural projection from the NL-recipient zone upon the contralateral NA-recipient zone in barn owls. Whether these discrepancies reflect significant functional and evolutionary divergence remains unknown.

The present study reconciles diverse studies in chicks, a worthy goal in view of its great utility in developmental and auditory studies and the availability of the chick genome. The organization of the afferent projections of the MLd was examined by placing anterograde and retrograde tracers into either the NA, the NL, or various locations of the MLd. These studies provide additional details of the organization of the chick MLd with an emphasis on the clarification of the characteristics of the third channel. This knowledge is prerequisite to understanding the relationship among time, intensity, and frequency processing at the midbrain level, as well as at later stages in the thalamus and telencephalon along the ascending pathway (Karten, 1967, 1968). Polysynaptic projections

TABLE 1.

Injection Sites in the NA, NL, and MLd and Tracers Used

Case	Injection site	Tracer
461	NL, NM	CTB
468	NL, NM	CTB
469	NL, NM	CTB
471	NL, NM	PHA-L
472	NL, NM	PHA-L
477	NL, NM	PHA-L
466	NA	CTB
480	NA	CTB
481	NA	CTB
483	NA	PHA-L
484	NA	PHA-L
419	Caudal MLd	CTB
327	Caudal MLd	CTB
339	Caudal MLd	CTB
322	Ventral MLd	CTB
323	Ventral MLd	CTB
324	Ventral MLd	CTB
333	Dorsal MLd	CTB
338	Dorsal MLd	CTB
340	Dorsal MLd	CTB
319	Central MLd	CTB
418	Rostromedial MLd	CTB

Abbreviations: NL, nucleus laminaris; NA, nucleus angularis; NM, nucleus magnocellularis; MLd, nucleus mesencephalicus lateralis pars dorsalis; CTB, cholera toxin B; PHA-L, *Phaseolus vulgaris*-leucoagglutinin.

from the NA and NL upon the MLd via the cell groups embedded in the lemniscus lateralis and the superior olive will be the topic of a future report.

MATERIALS AND METHODS

Experiments were performed on White Leghorn chick hatchlings less than 5 days old (*Gallus gallus*). The general organization of the auditory pathway is considered to be stabilized after hatching (for review, see Rubel and Parks, 1988). All experimental procedures were approved by the University of California, San Diego Animal Care Committee and conformed to the guidelines of the National Institutes of Health on the Care and Use of Laboratory Animals.

In vivo CTB and PHA-L tract tracing

Chicks were anesthetized with a mixture of 40 mg/kg ketamine and 12 mg/kg xylazine and placed in a stereotaxic head holder. The skull was exposed and a hole was made above the injection target area estimated from stereotaxic coordinates (Kuenzel and Masson, 1988). A solution of 1% cholera toxin B-subunit (CTB; List Laboratories, Campbell, CA) was injected through a glass micropipette by using a pressure device (PicoSpritzer II; General Valve, Fairfield, NJ). In a separate group of subjects, *Phaseolus vulgaris*-leucoagglutinin (PHA-L; Vector, Burlingame, CA) was iontophoretically deposited by means of glass micropipettes with a tip diameter of 2–10 μm and filled with
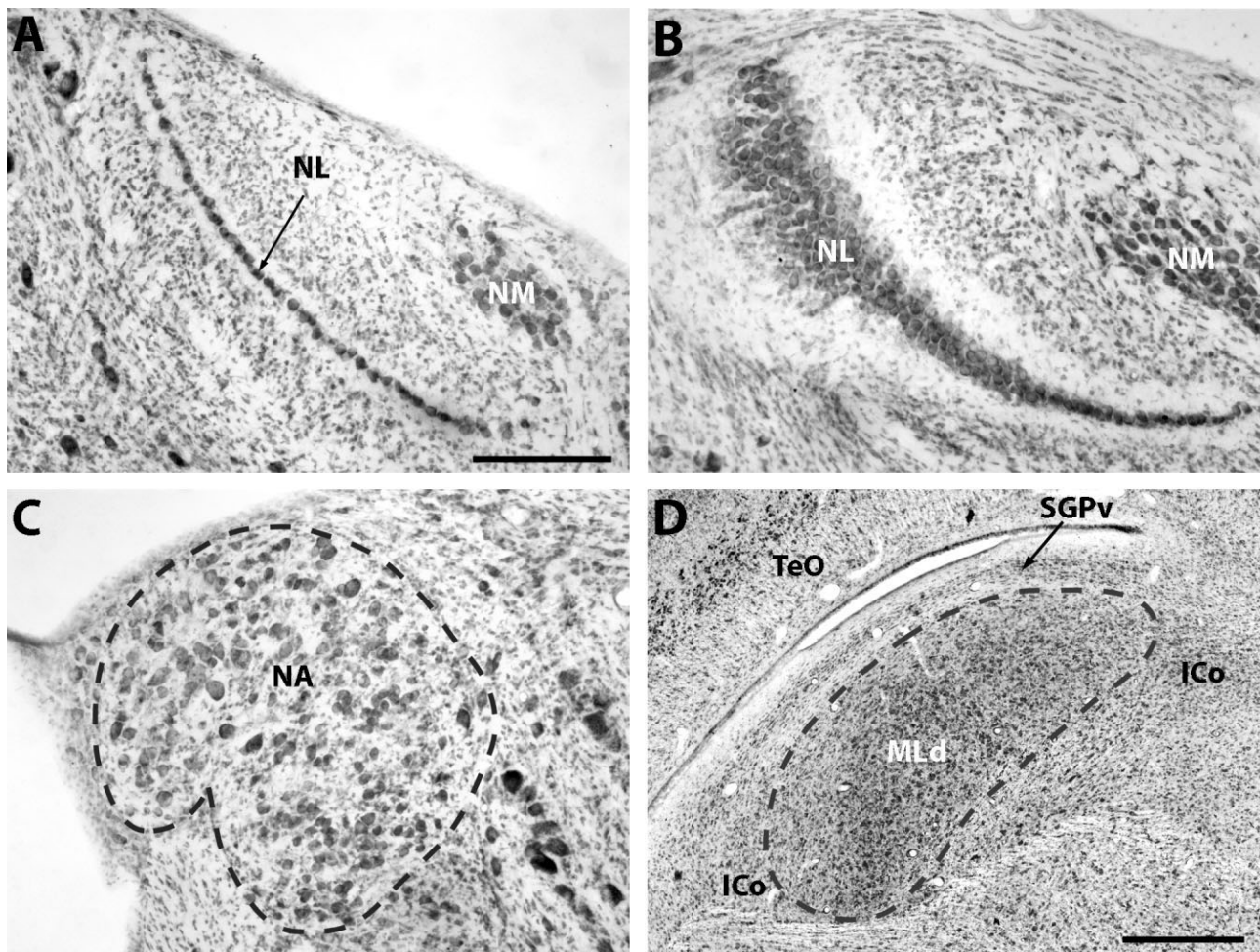
Figure 1. The chick NL at intermediate (**A**) and caudal (**B**) levels, NA (**C**), and MLd (**D**) in Nissl-stained sections in the coronal plane. Dashed lines in C and D indicate the outlines of NA and MLd, respectively. Abbreviations: NL, nucleus laminaris; NA, nucleus angularis; NM, nucleus magnocellularis; MLd, nucleus mesencephalicus lateralis pars dorsalis; TeO, optic tectum; SGPv, stratum griseum periventriculare; ICo, nucleus intercollicularis. Scale bar = 200 μm in A (applies to A–C); 500 μm in D.

a solution of 2.5% PHA-L. The parameters of iontophoretic injection were a constant positive current of 2–10 μA for 10 minutes to deposit a small amount of tracer. The site of each successful injection, as well as the tracer used in each case, is listed in Table 1. Following CTB or PHA-L injections, the micropipette was retracted, the wound was closed, and the animal was allowed to recover. After a survival time of 3 days, animals were transcardially perfused with 0.9% saline followed by chilled 4% paraformaldehyde in phosphate buffer (PB; 0.1 M, pH 7.2–7.4). The brains were removed from the skull, postfixed overnight in the same paraformaldehyde solution, and then transferred to 30% sucrose in PB until they sank. Each brain was frozen and cut coronally at 30 μm on a freezing sliding microtome, and each section was collected in phosphate-buffered saline (PBS; 0.1 M, pH 7.2–7.4).

Standard immunohistochemistry procedures were applied to reveal the distribution of CTB and PHA-L. Briefly,

sections were incubated with primary antibody solution diluted in PBS (anti-CTB, 1:12,000; anti-PHA-L, 1:1,000) with 0.3% Triton X-100 overnight at 4°C, followed by biotinylated IgG antibodies (1:200; Vector) for 1 hour at room temperature. Polyclonal anti-CTB made in goat, purchased from List Laboratories (lot no. 703), was raised against unconjugated, purified cholera toxin B subunit isolated from *Vibrio cholerae*. Anti-PHA-L, purchased from Vector (cat. no. AS-2300), was produced by hyperimmunizing rabbits with pure lectins. Following conventional purification steps, specific antibody was isolated by affinity chromatography on lectin-agarose columns. Sections were then incubated in avidin-biotin-peroxidase complex solution (ABC Elite kit; Vector) diluted 1:100 in PBS with 0.3% Triton X-100 for an hour at room temperature. Sections were incubated for 3–5 minutes in 0.025% 3-3′-diaminobenzidine (DAB; Sigma, St. Louis, MO) with 0.01% hydrogen peroxide in PB. Sections were mounted on gelatin-coated slides and were
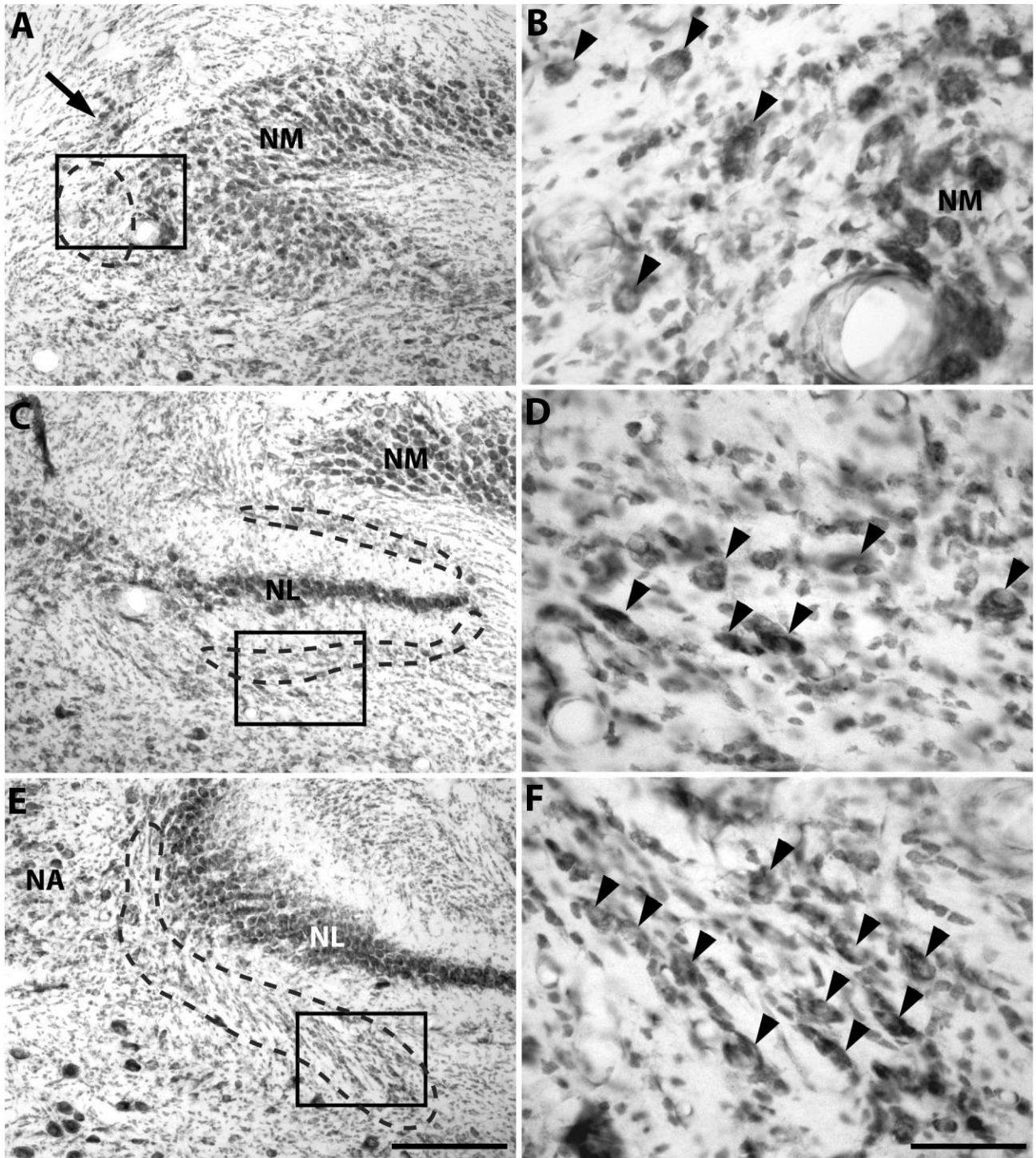
Figure 2. Three neuronal clusters, termed RI in the current study, in Nissl-stained sections in the coronal plane. **A,C,E:** Low-power images illustrating approximate location of the clusters (dashed lines) and their relationship to NM/NL/NA. Loose packing, light staining, and their location adjacent to NM/NL/NA of these clusters do not allow us to draw their exact boundaries. Images from A to E represent sections at the levels from caudal to rostral, although they were all caudal to the level in Figure 1B. Arrow in A points to a neuronal cluster with more prominent Nissl staining than that in RI. No retrogradely labeled neurons in this cluster were found following injections into the MLd. **B,D,F:** High-power images of the boxed regions in A, C, and E, respectively. Arrowheads indicate neuronal cell bodies in each cluster. Note many neurons in F are elongated and oriented parallel to the long axis of the cluster. For abbreviations, see Figure 1 legend. Scale bar = 400 μm in E (applies to A,C,E); 100 μm in F (applies to B,D,F).
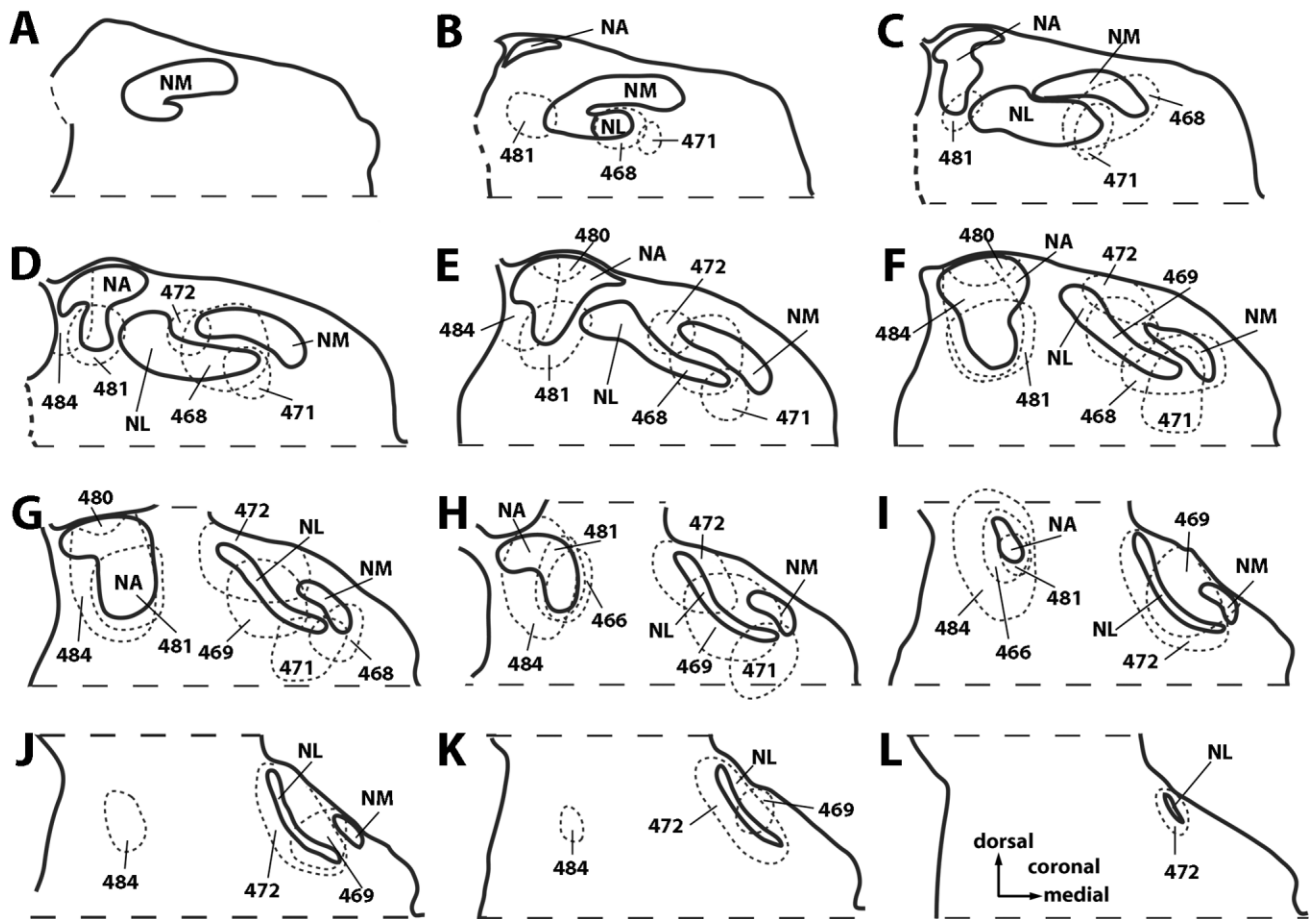
Figure 3. Injection sites in NA (cases 466, 480, 481, and 484) and NL (cases 468, 469, 471, and 472). **A–L:** Drawings represent sections at the levels from caudal to rostral. Dashed circles indicate injection sites that are defined as the blackened region in a section under brightfield observation. As an example, case 469 at the level of H was drawn from the section illustrated in Figure 5A. Injection sites of cases 461, 477, and 483 largely overlap with those of cases 469, 468, and 481, respectively, and are not included in the drawing for clarity of the figure. For abbreviations, see Figure 1 legend.

either stained with 0.05% osmium tetroxide for 30 seconds or counterstained with Giemsa (Iñiguez et al., 1985). Sections were then dehydrated, cleared, and coverslipped with Permount (Fisher Scientific, Pittsburgh, PA). To test the specificity of the primary antibodies further, sections were prepared from an animal that did not receive an injection with either CTB or PHA-L, and probed immunohistochemically with these antibodies. No specific staining was detected in any brain regions, compared with control sections that were probed without the primary antibodies.

Imaging and cell counting

All CTB- or PHA-L-labeled neurons and terminals were reconstructed with a camera lucida on a Zeiss WL microscope (Carl Zeiss, Thornwood, NY). The drawings were then digitized and edited in Canvas (Deneba Systems, Miami, FL). Digital images of selected sections were captured with a Nikon D100 digital camera mounted on a Nikon photomicroscope (Nikon, Tokyo, Japan) or a Phase One

FX+ digital studio camera system (Phase One A/S Denmark, Frederiksberg, Denmark). Image contrast adjustments and photomontages were performed by using Adobe Photoshop (Adobe Systems, Mountain View, CA).

Labeled neurons were counted and the somatic area was measured in Image J software (version 1.38X; National Institutes of Health). Data are shown as mean $\pm$ 1 SD in the text. Labeled neurons without an obvious nuclear profile were excluded from counting and measuring. Abercrombie's formula was used to correct cell profile counting in each group (Table 2), except for that in the NM, where only two labeled neurons were found.

$$N = \frac{T}{T+D} \times n$$
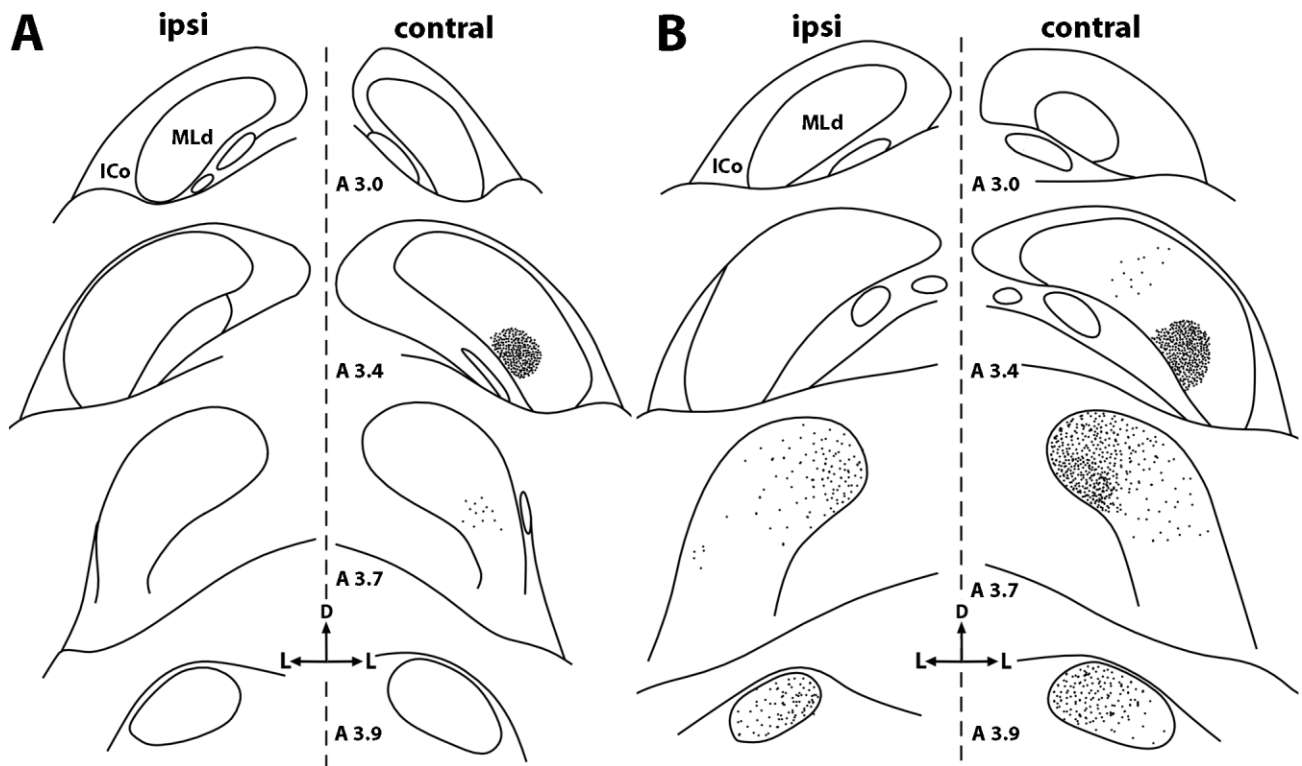
Figure 4. Line drawings of two different patterns of anterograde labeling in the MLd following injections into the NL/NM. **A:** Anterograde terminals were found contralaterally in a small central region along the medial border of the MLd. The injection site is illustrated in Figure 3 (case 469). **B:** Anterograde terminals were detected bilaterally in the rostromedial portion of the MLd, in addition to the small central region. The injection site is illustrated in Figure 3 (case 471). Black dots represent anterograde terminals. Numbers below each drawing indicate the approximate anterior-posterior stereotaxic levels. For abbreviations, see Figure 1 legend.

where N = number of cells, T = section thickness, D = mean of diameters of 12 nuclei, and n = number of counted nuclei.

RESULTS

Figures 1 and 2 illustrate the location and general organization of the major nuclei examined in the current study in Nissl-stained sections. In chicks, the NL is located ventrolaterally and rostrally to the NM, with its neurons arranged in a single layer (Fig. 1A), except in its caudolateral region, where multilayers of neurons are present (Fig. 1B). The NA is a heterogeneous cell group located laterally and caudally to the NL (Fig. 1C; Soares et al., 2002). The MLd is situated in the caudal midbrain below the tectal ventricle, and surrounded by the nucleus intercollicularis and the stratum griseum periventriculare (Fig. 1D; Karten, 1967; Puelles et al., 1994).

In addition, scattered neurons and/or small neuronal clusters are identified in the surrounding region lying between the NM, NL, and NA at the caudal level. These neurons are less prominent in Nissl-stained sections compared with the NM/NL/NA due to their loose packing and light staining. Three such neuronal clusters that

contained retrogradely labeled neurons following injections into the MLd are illustrated in Figure 2. The first cluster is located lateral to the NM at the level caudal to the NL (Fig. 2A,B). In some sections, the distribution of these neurons appears to extend medially along the ventral edge of the NM. The second cluster is a group of scattered neurons distributed along the outer edge of the ventral neuropil of the NL (Fig. 2C,D). Although they are seen less frequently, some neurons are also found along the outer edge of the dorsal neuropil of the NL. The third cluster extends from the gap between the NL and the ventral NA and sweeps ventrally and medially (Fig. 2E,F). Many neurons in this region display an elongated cell body oriented parallel to the long axis of the cluster. Complete separation of these three neuronal clusters from each other and from surrounding regions in Nissl-stained sections is impractical as these clusters appear to be continuous with each other and located immediately adjacent to the NM, NL, and NA. As described below, these three neuronal clusters are the most prominent groups beyond the boundaries of the NM, NL, and NA that contain retrogradely labeled neurons following injections into the MLd. To facilitate fur-
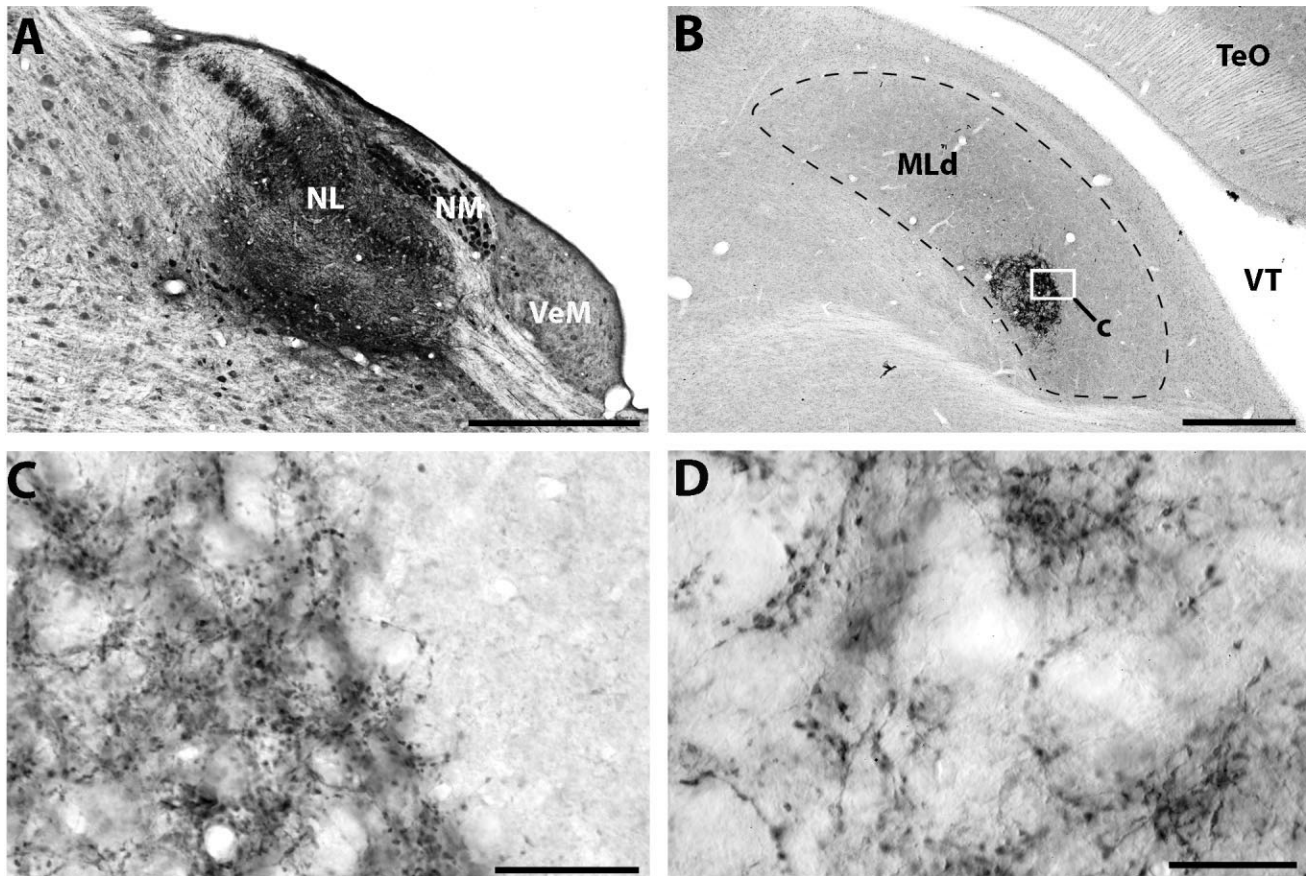
Figure 5. Brightfield photomicrographs of anterograde labeling in the MLd following an injection of CTB into the NL (case 469). **A:** The injection site in the NL. **B:** The restricted distribution of the anterograde labeling within the contralateral MLd. **C:** A closer view of the box in B illustrating the sharp edge formed by labeled terminals from adjacent unstained area. **D:** A high-magnification photo showing terminal clusters. A was taken from a Giemsa-counterstained section and B–D from non-counterstained sections. Abbreviations: VeM, nucleus vestibularis medialis; VT, ventriculus tecti mesencephali. For abbreviations, see Figure 1 legend. Scale bar = 500 µm in A,B; 50 µm in C; 30 µm in D.

ther description, we designate them collectively as the *regio intermedius* (RI) based on their location.

Injections of CTB or PHA-L into the NL

For injections into the NL, the micropipette was inserted vertically through the overlying cerebellum into the NL. To avoid the micropipette passing through or the tracer diffusing into the adjacent NA, the injections specifically avoided a small portion of the caudolateral NL that is immediately ventral and medial to the NA (Fig. 3). Other than that, different injections in the NL covered the whole nucleus throughout its rostrocaudal and mediolateral extents. In addition, every injection into the NL involved a portion of the NM (Fig. 3).

Following injections into the NL and NM, the distribution pattern of anterograde labeling within the MLd falls into two groups. In the first group, anterogradely labeled terminals within the MLd were found mostly, if not exclusively, contralaterally (Fig. 4A). These terminals were highly concentrated in a small central, although relatively ventral,

region along the medial border of the nucleus at the intermediate level (Fig. 5B). Remaining areas were totally lacking labeling (Fig. 5C), except for a very low density of scattered terminals in the rostral MLd. Labeled terminals in the MLd often formed clusters with axonal bouton-like swellings (Fig. 5D). Cases in the first group tended to have a relatively restricted injection in the NL/NM region and did not involve the most caudal portion of the NL or neuronal clusters in the RI. Cases 469 and 472 in Figure 3 represent such examples.

The second group exhibited anterogradely labeled terminals bilaterally in the rostromedial portion of the MLd, in addition to the small central region of the contralateral MLd (Fig. 4B). Labeled terminals in these two regions were discontinuous from each other, a pattern especially evident in the cases with heavy staining. The density of labeled terminals in the rostromedial MLd was consistently higher on the side contralateral to the injection than on the other side. Injection sites of the second group either extended ventrally across the fiber bundle deep into the ven-
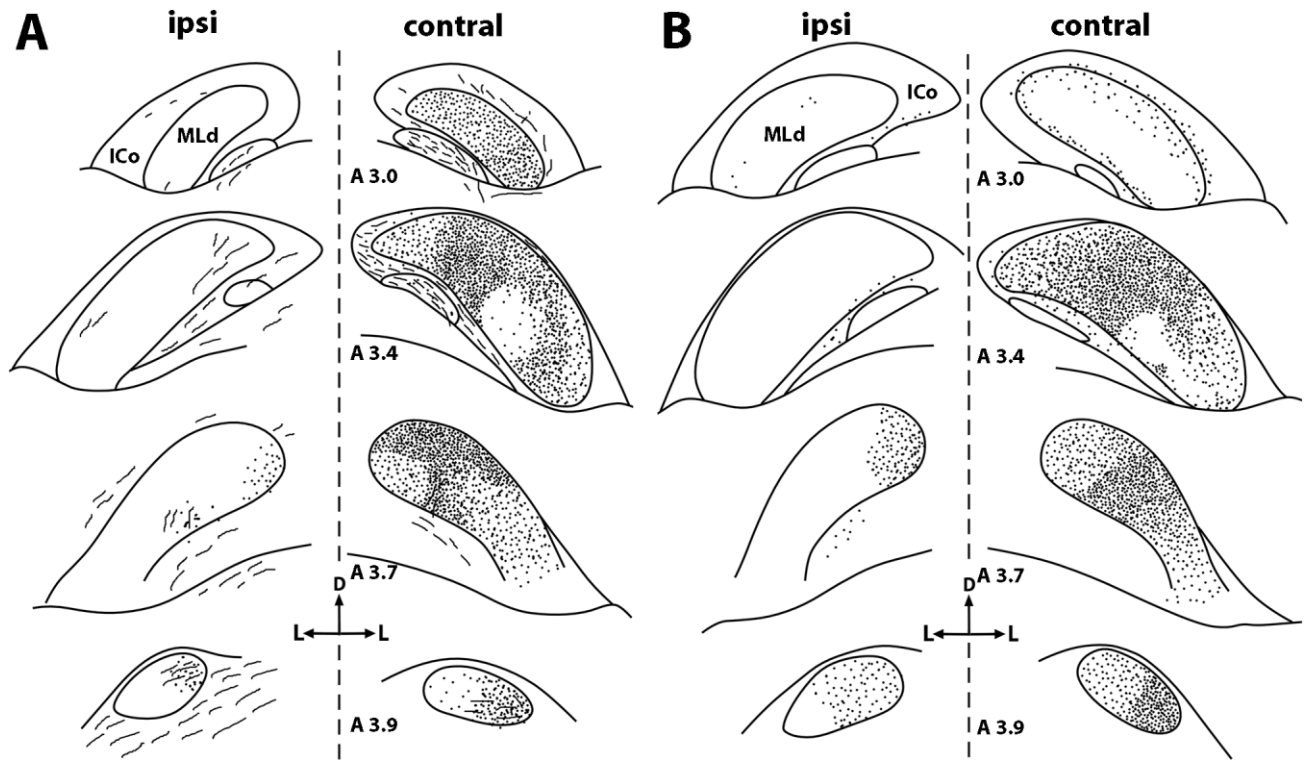
Figure 6. Line drawings of anterograde labeling in the MLd following injections into the NA. **A:** Labeled terminals were distributed heterogeneously throughout the contralateral MLd and within the rostromedial portion of the ipsilateral MLd. Within the contralateral MLd, a small central region along the medial border of the nucleus contained the lowest density of labeling. The injection site is illustrated in Figure 3 (case 484). **B:** Anterogradely labeled terminals in the contralateral MLd were sparser in the caudal and caudoventral portion than in the dorsal and lateral portion of the nucleus following an injection in the ventral NA. The injection site is illustrated in Figure 3 (case 481). Black dots represent anterograde terminals. Short lines in A indicate PHA-L-labeled fiber fragments. Numbers below each drawing indicate the approximate anterior-posterior stereotaxic levels. For abbreviations, see Figure 1 legend.

tral vestibular nuclei and/or encroached on the most caudal region of the NL and the surrounding area. Cases 468 and 471 in Figure 3 represent such examples.

Injections of CTB or PHA-L into the NA

For injections into the NA, the micropipette went tangentially from the cerebellum across the midline and into the contralateral NA. Different injections in the NA covered the whole nucleus except for its most caudodorsal portion (Fig. 3). Most injections into the NA did not involve the NL, except in one case, in which the tracer diffused into a very small portion of the caudal NM and NL (case 481 in Fig. 3). This case also involved neuronal clusters in the RI.

Injections into the NA produced a similar distribution of anterograde labeling within the MLd in all cases (Fig. 6; except for case 480). On the side contralateral to the injection, labeled terminals were found extensively and widely within the MLd. The terminal density varied in relationship to the injection site within the NA. Following an injection concentrated in the ventral portion of the NA, labeled terminals were substantially denser in the dorsal and lateral portion than in the caudal and caudoventral portion of the MLd (Figs. 6B, 7A,B), whereas injections involving both the dorsal and ventral NA produced a relatively uniform distribution of labeling in the MLd (Fig. 6A). However, a small central region along the medial border of the nucleus consistently contained the sparsest terminals (Fig. 7B,C), whose location approximately corresponds to where dense NL terminals were found. The density of labeled terminals in the rostromedial portion of the nucleus was also consistently lower than the adjacent ventral portion (Figs. 6, 7D,F).

On the side ipsilateral to the injection, anterograde labeling was predominantly concentrated in the rostromedial portion of the MLd (Figs. 6, 7E), with occasional terminals scattered in other portion of the nucleus. As a result, a boundary between the rostromedial and other portions of the MLd could be easily drawn, as the terminal density in the rostromedial MLd was substantially lower on the side contralateral to the injection, and was significantly higher on the side ipsilateral to the injection, compared with the adjacent ventral region (Fig. 7D–F).
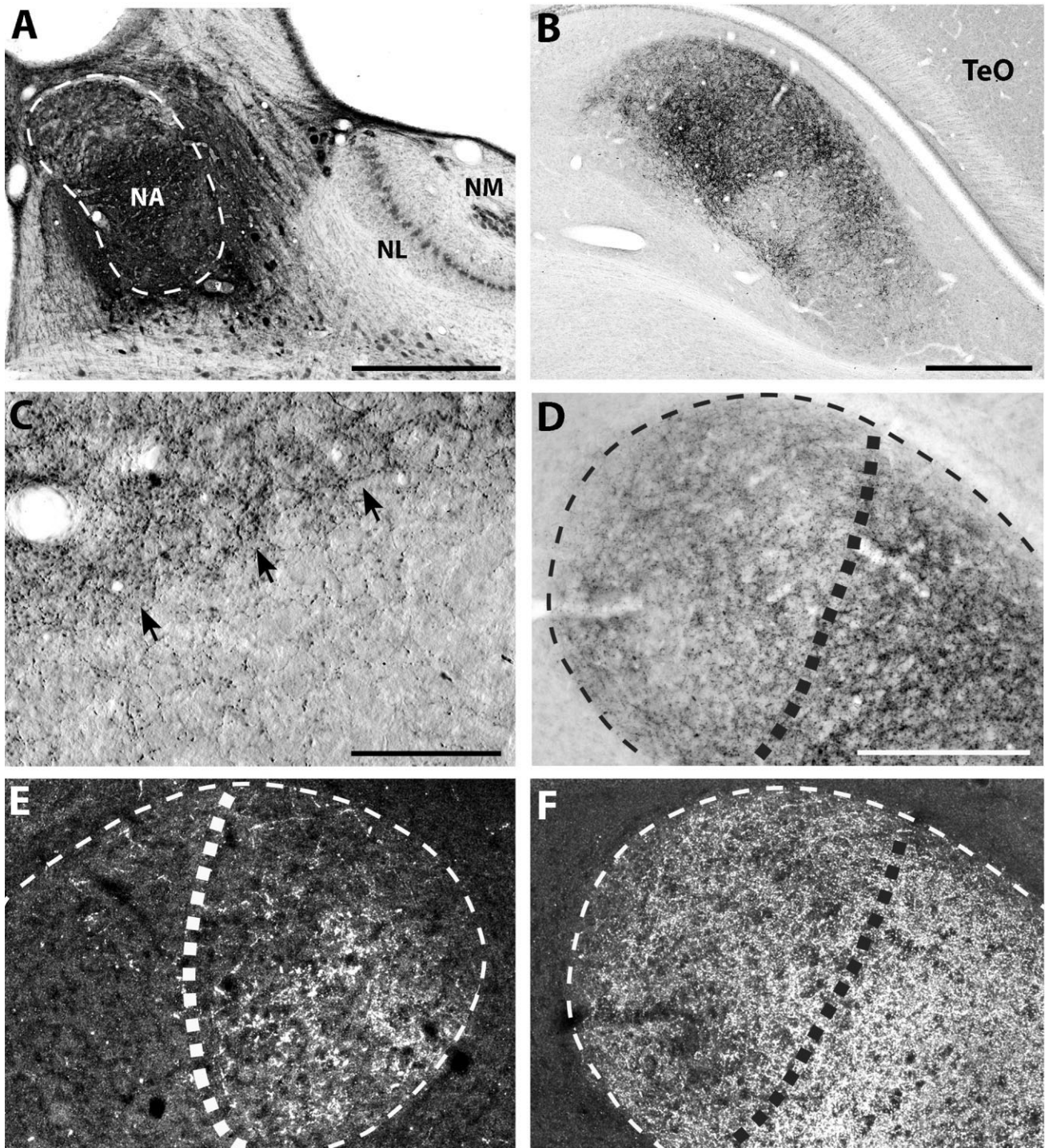
Figure 7. Photomicrographs of anterograde labeling in the MLd following an injection of CTB into the NA (case 481). **A:** The injection site in the NA. Dashed lines indicate the boundary of the NA **B:** Widely distributed anterograde labeling in the contralateral MLd. **C:** Abrupt changes in the density of labeled terminals (arrows) between the small central region and the surrounding area. **D:** Brightfield image of the rostromedial portion of the contralateral MLd. **E–F:** Darkfield images of the rostromedial portion of the ipsilateral (E) and contralateral (F) MLd. Dashed lines in D–F indicate the boundaries of the MLd. Note changes in the density of labeled terminals between the rostromedial portion and the adjacent ventral region (thick dotted lines). A was taken from a Giemsa-counterstained section and B–F from non-counterstained sections. D and F were taken from the same section. For abbreviations, see Figure 1 legend. Scale bar = 500 μm in A,B; 100 μm in C; 500 μm in D (applies to D–F).
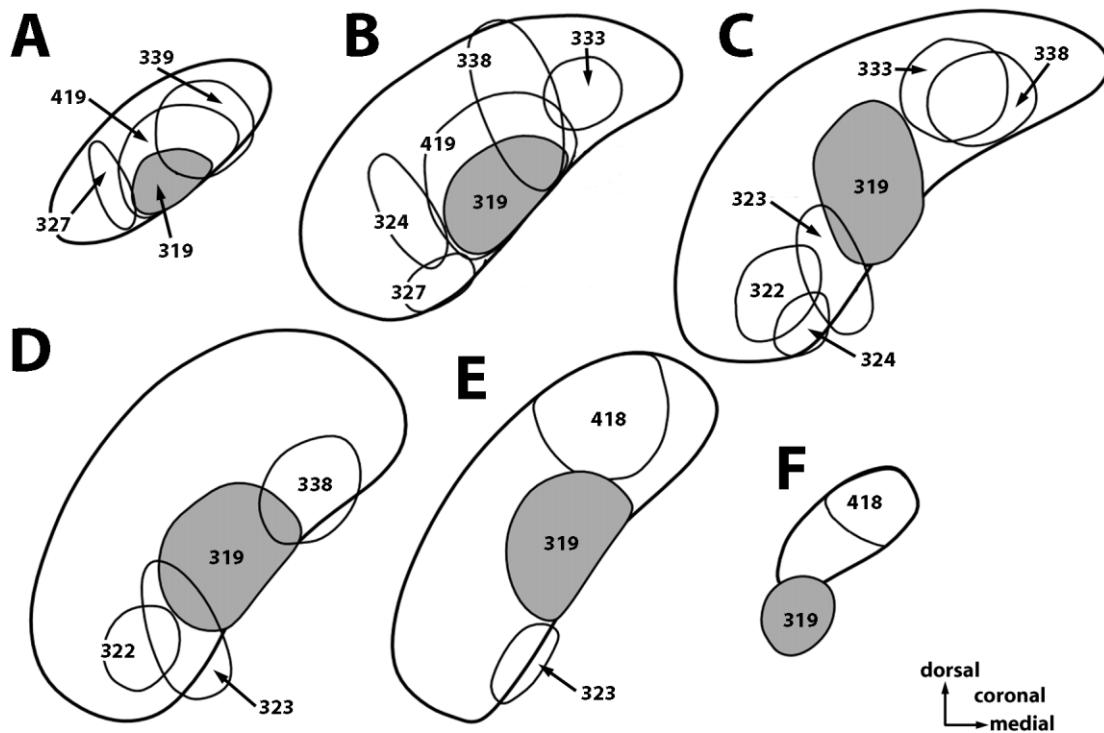
Figure 8. Injection sites in MLd. **A–F:** Drawings represent sections at the levels from caudal to rostral. Case 319 is an injection that involved the major portion of the NL-recipient zone and is illustrated in gray to distinguish from other cases.

The injection in case 480 involved only a very small portion of the dorsal NA and produced sparse antero-gradely labeling in the MLd. Although labeled terminals were found in different regions of the nucleus, specific patterns of distribution cannot be determined.
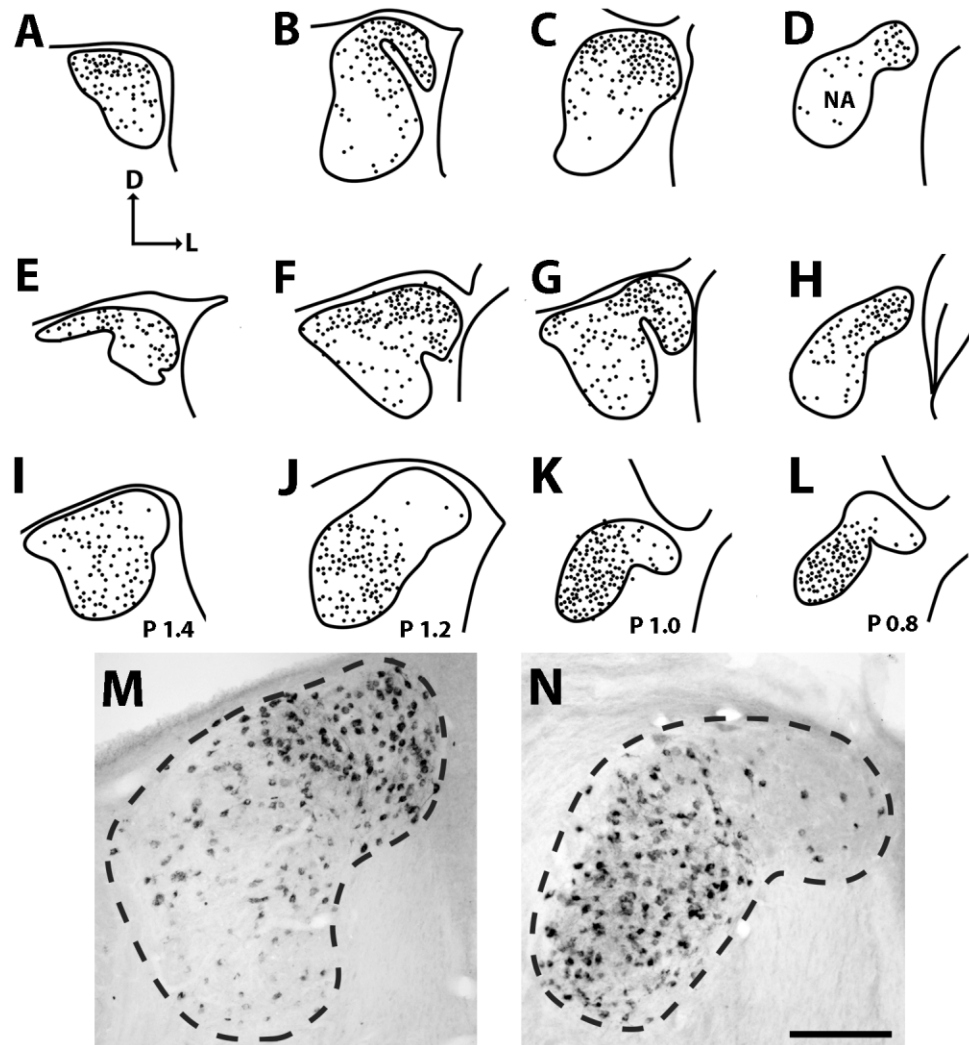
Injections of CTB into the MLd

Retrograde labeling in the caudodorsal brainstem

Regardless of the injection sites within the MLd (Fig. 8), retrogradely labeled neurons were found in both the NA and NL, although the percentage of labeled neurons in each nucleus varied across cases. This may be due to a substantial mixture of afferent fibers from the NA and NL within the MLd, or alternately, may reflect the difficulty of obtaining injections limited to sufficiently restricted re-gions of the MLd. On the other hand, these retrograde tracing studies confirmed that the projections from the NA and NL upon the majority of the MLd (except for its rostro-medial portion) are mostly, if not exclusively, contralater-ally. Statistical analyses among all cases with injections into the MLd (excluding case 418 with an injection in the rostromedial portion) demonstrated that the percentage of labeled neurons on the ipsilateral side was 2.9 ± 2.3% (n = 10; ranging from 0.3% to 6.6%) in the NA and 2.8 ± 4.2% (n = 10; ranging from 0 to 10.7%) in the NL. In addition,

distributions of labeled neurons within the contralateral NA support the topography of the projection from the NA upon the MLd. Injections into the caudal or ventral portion of the MLd retrogradely labeled neurons mainly in the dor-sal NA, whereas the majority of neurons were found in the ventral NA following injections into the dorsal MLd (Fig. 9). No labeled neurons were found in the NM.
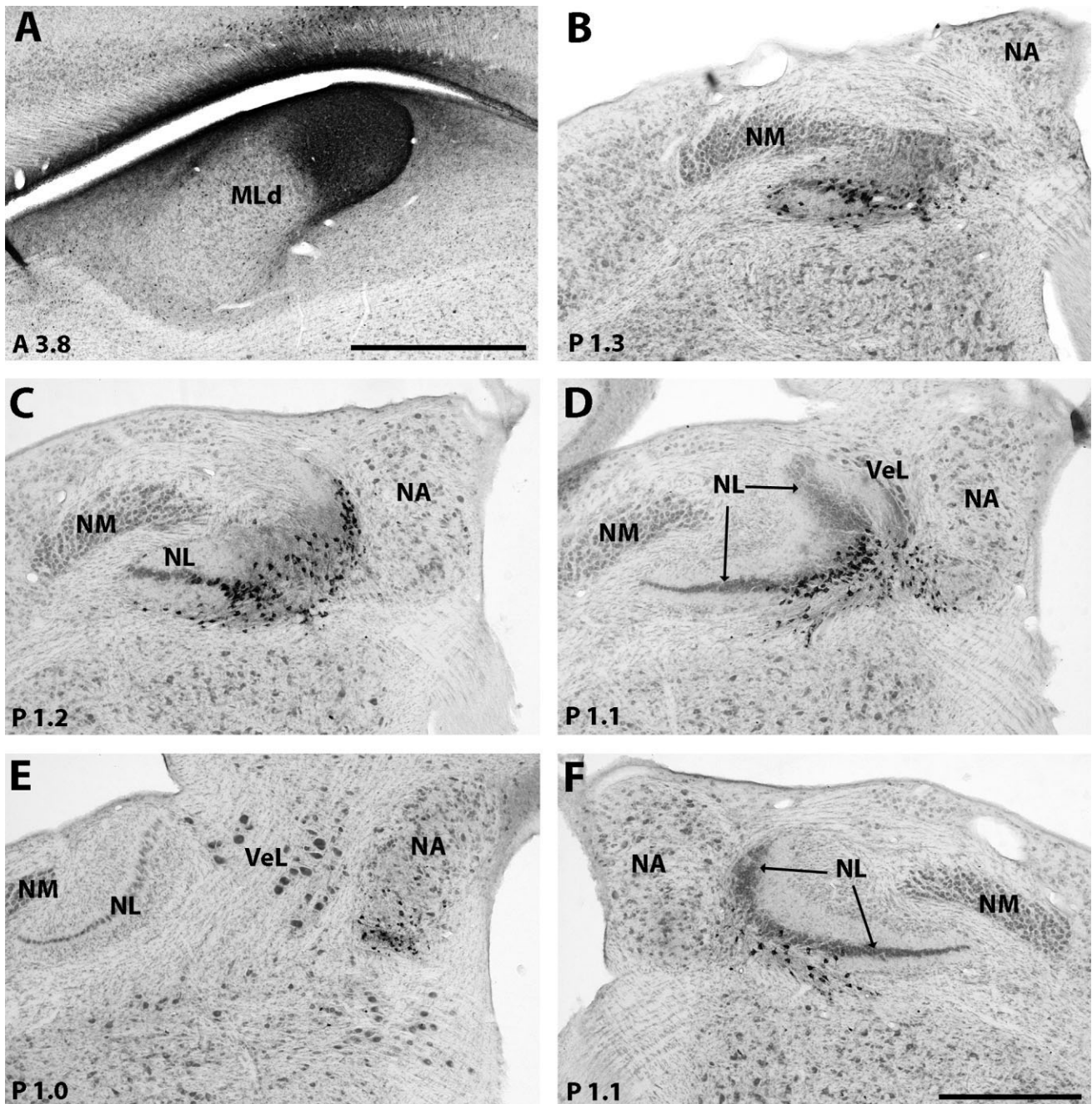
An injection into the rostromedial portion of the MLd (case 418) clarified the nature of the bilateral inputs to this region (Figs. 10,11). Retrogradely labeled neurons in the caudodorsal brainstem were found bilaterally and symmet-rically in the caudal NL, the ventral NA, and neuronal clus-ters in RI. Labeled neurons in the caudal NL were mostly located in the multilayered portion and predominantly on the side contralateral to the injection (Figs. 10C,D, 11D–F). The average soma area was 196 ± 37 μm^2 (n = 29). Labeled neurons in the NA were located along the ventro-medial edge of the NA at the caudal level (Figs. 10D, 11E) and concentrated in the very ventral region of the nucleus throughout the intermediate and rostral levels (Figs. 10E, 11H,I). The majority of these neurons were small, with an average soma area of 114 ± 31 μm^2 (n = 86). All three neuronal clusters of the RI that we identified in Nissl-stained sections contained a substantial number of la-beled neurons (Fig. 11A–F). A few labeled neurons were also found in surrounding areas beyond these clusters (Fig.

Figure 9. Line drawings and photomicrographs of the distribution of retrogradely labeled neurons in the contralateral NA following injections into the caudal (**A–D**, case 419), ventral (**E–H,M**, case 322), or dorsal (**I–L,N**, case 333) portions of the MLd. Most of the retrogradely labeled neurons were situated in the dorsal NA following injections into the caudal or ventral portion of the MLd, and in the ventral NA following an injection into the dorsal portion of the MLd. Black dots in A–L represent retrogradely labeled neurons. Dashed lines in M and N indicate the boundaries of the NA. Numbers below each lane of drawings indicate the approximate anterior-posterior stereotaxic levels. NA, nucleus angularis. Scale bar = 200 μm in N (applies to M,N).

11G). Some of these neurons were located clearly beyond the boundaries that delimit the major body of the NM, NL, and NA, whereas others were distributed along the edges of these nuclei so that we were not able to determine unambiguously whether they belongedo one of these three nuclei. The soma area of these neurons and labeled neurons in the RI varied greatly and averaged $134 \pm 57 \ \mu m^2$ (n = 176). In addition, a number of labeled neurons were identified in the region ventral to the NM/NL/NA/RI complex (Fig. 11J). They were embedded among large cell bodies of vestibular neurons and often located along the tract of the 8th nerve (Fig. 11K,L). They had very small cell bodies with a soma area of $80 \pm 21 \ \mu m^2$ (n = 43) and did not form clusters as in the RL.

To determine whether these labeled neurons provide bilateral projections to the rostromedial MLd or whether some of them were labeled due to tracer diffusing into regions of the MLd that are mainly innervated by the contralateral projections from the NL and NA, we counted the number of labeled neurons in each cell group on each side. Because injections into other regions of the MLd produced an average of 3% neurons on the ipsilateral side of the NL and NA, if a certain cell group in case 418 was labeled due to tracer diffusion into these regions, we expected to see a small percentage (~3%) of labeled neurons on the ipsilateral side. In general, the density of labeled neurons was substantially lower on the ipsilateral side than on the contralateral side. Specifically, the percentage of labeled neu-

Figure 10. Retrogradely labeled neurons in the caudodorsal brainstem following a CTB injection into the rostromedial portion of the MLd (case 418). **A:** The injection site in the rostromedial portion of the MLd. **B–E:** Series of sections through the contralateral NM, NA, and NL. **F:** A section through the ipsilateral NM, NA, and NL. Note retrogradely labeled neurons were not located in the major body of the NL or NA. Approximate anterior-posterior stereotaxic levels are indicated at the lower left corner of each photo. Images were taken from Giemsa-counterstained sections. For abbreviations, see Figure 1 legend. Scale bar = 1 mm in A; 500 μm in F (applies to B–F).

rons on the ipsilateral side among the total on two sides was 2.9% in the NL, 7.3% in the NA, 21.6% in the RI, and 49.2% in the region ventral to the NM/NL/NA/RI complex and within the 8th nerve tract (Table 2). This analysis indicates that the RI and scattered neurons along the 8th nerve tract, and probably the ventral NA, do indeed send bilateral inputs to the rostromedial MLd. Labeled neurons

in the NL have a low percentage of distribution on the ipsilateral side, which does not support a bilateral projection from this region to the midbrain.

In addition, we detected two labeled neurons that appeared to be located within the caudoventral NM on the contralateral side (Fig. 11C). Both neurons were located close to the periphery, which may reflect the fact that the
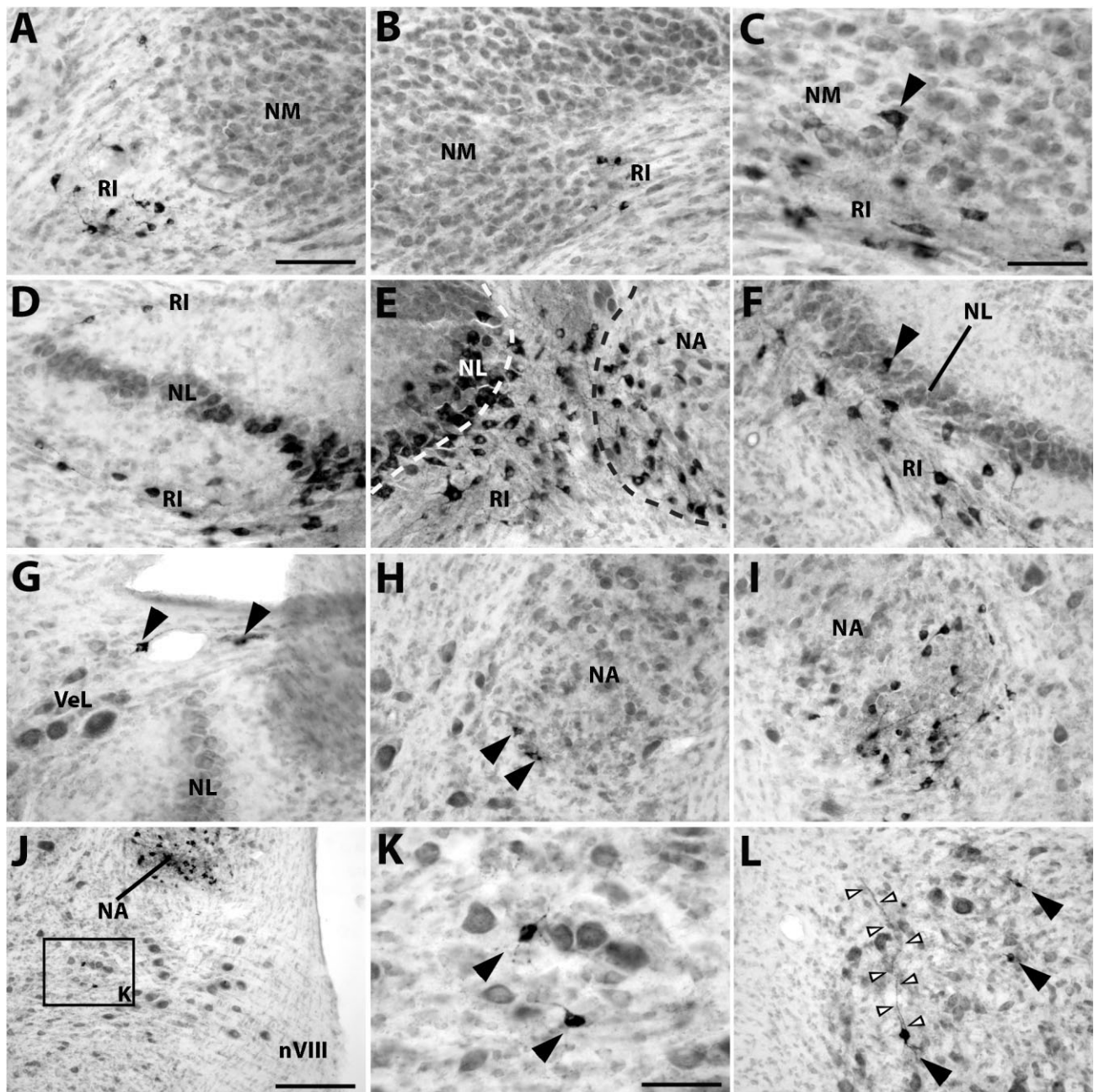
Figure 11. High-magnification photomicrographs of labeled neurons following injection into the rostromedial portion of the MLd (case 418). **A,B:** Labeled neurons in the neuronal cluster depicted in Figure 2A on the ipsilateral side. **C:** One labeled neuron (arrowhead) that appeared to be located within the caudoventral region of the contralateral NM. **D:** Labeled neurons in the neuronal cluster depicted in Figure 2C on the ipsilateral side. **E,F:** Labeled neurons in the neuronal cluster depicted in Figure 2E on the contralateral (E) and ipsilateral (F) side. **G:** Two scattered neurons (arrowheads) labeled in the surrounding region. **H,I:** Labeled neurons in the ventral region of the NA on the ipsilateral (H) and contralateral (I) side. **J–L:** Labeled neurons in the region ventral to the NA on the contralateral (J,K) and ipsilateral (L) side. Arrowheads in K and L point out labeled neurons. K is a closer view of the box in J. Empty arrowheads in L indicate the course of one axonal collateral of a labeled neuron. All images were taken from Giemsa-counterstained sections. Up is dorsal. Right is medial and lateral for images taken from the ipsilateral and contralateral side, respectively. Abbreviations: RI, regio intermedius; VeL, nucleus vestibularis lateralis; nVIII, 8th nerve. For other abbreviations, see Figure 1 legend. Scale bar = 100 μm in A (applies to A,B,D–I,L); 50 μm in C,K; 200 μm in J.

NM, NL, and NA are not sharply and absolutely delineated from each other and from the surrounding area, at least in chick hatchlings, and may not indicate that the NM projects to the midbrain.

Commissural connections of the MLd

The topography of commissural connections of the MLd was mapped following unilateral injections in various locations of the MLd. To facilitate the description of this topog-

TABLE 2.

Numbers of Labeled Neurons in the NM, NL, NA, RI, and the Region Ventral to the NM/NM/NA/RI Complex Following Injection Into the Rostromedial MLd (Case 418)[1]

	No. of labeled neurons		Ipsilateral/ (Contralateral Ipsilateral) (%)
Site	Contralateral	Ipsilateral	
Caudoventral NM	2	0	0
Caudolateral NL	100	3	2.9
Ventromedial and ventral NA	101	8	7.3
RI and scattered neurons in surrounding regions	174	48	21.6
Region ventral to the NM/NL/NA/RI complex	30	29	49.2

[1]Numbers of labeled neurons on each side (contralateral and ipsilateral) are listed separately. The percentages of labeled neurons on the ipsilateral side among all labeled neurons are calculated. Neurons whose location cannot be unambiguously determined are grouped into the fourth category. Abbreviations: NL, nucleus laminaris; NA, nucleus angularis; NM, nucleus magnocellularis; MLd, nucleus mesencephalicus lateralis pars dorsalis; RI, region intermedius.

raphy in relationship to the organization of the ascending projections from the NA and NL, we termed the small central region along the medial border of the MLd the *NL-recipient zone*, as it is innervated predominantly by the contralateral NL. The rostromedial portion of the MLd receives bilateral inputs from the caudodorsal brainstem, and is designated the *bilateral zone*. The remaining region of the MLd in receipt of the contralateral NA is designated the *NA-recipient zone*.

The NA-recipient zone is the largest subdivision of the MLd. Our injections into this subdivision usually only involved a portion of it and could be organized into three groups, the ones concentrated in the caudal, ventral, or dorsal portions. Injections in all three groups displayed a similar distribution pattern of retrograde and anterograde labels in the contralateral MLd. Retrogradely labeled neurons were widely distributed, with the predominant population in the NL-recipient zone (Figs. 12, 14A). Anterogradely labeled neuropil was distributed mainly along the dorsal, lateral, and ventral borders of the nucleus rather than within the major body in receipt of the NA.

In contrast, the NL-recipient zone occupies a small volume of the nucleus; our injection centered in the NL-recipient zone involved a substantial portion of the adjacent NA-recipient zone. In the contralateral MLd, anterogradely labeled terminals were found extensively in the NA-recipient zone (Figs. 13, 14B). These terminals were not uniformly distributed, with the highest density in the dorsal portion. Notably, neurons in the contralateral NL-recipient zone were densely labeled. However, this region was lacking anterogradely labeled terminals (Fig. 14C), demonstrating that the two NL-recipient zones were not reciprocally connected. These neurons were probably labeled due to the tracer spreading into the adjacent NA-recipient zone. Retrogradely labeled neurons were also found in the bilateral zone of the MLd.

Following an injection into the bilateral zone of the MLd (case 418; Fig. 15), the NL- and NA-recipient zones on the contralateral side were totally lacking any retrograde or anterograde labeling. Labeled neurons and neuropil densely overlapped in the contralateral bilateral zone (Fig. 14D). This pattern indicates that labeled neurons in the bilateral zone following injections in the NA- or NL-recipient zone described above were due to tracer spreading directly into the bilateral zone, or else they were inadvertently labeled by fibers of passage. In addition, a prominent bundle of fibers was labeled along the rostrolateral margin of the nucleus.

These results demonstrate a heavy commissural projection from the NL-recipient zone upon the contralateral NA-recipient zone and a highly restricted reciprocal connection between the bilateral zones of two sides. Neurons in the NA-recipient zone of the MLd may also send their axons contralaterally, and thus distributed mainly along the borders of the MLd.

DISCUSSION

The current study has identified three subdivisions of the MLd in chicks based on the organization of their afferent and commissural projections. The main results are summarized and schematically illustrated in Figure 16. These results, as well as a comparison with the data from other avian species and mammals, may contribute to a better understanding of the organization and function of the auditory midbrain.

Three ascending auditory pathways to the midbrain

One of the most common features of auditory information processing in birds is that acoustic information is conveyed to the midbrain in at least two separate ascending pathways from the NA and NL upon two non-overlapping subdivisions of the contralateral MLd (barn owl: Takahashi and Konishi, 1988a; chicken: Conlee and Parks, 1986; pigeon: Leibler, 1975; Wild, 1995). Both the NA and NL con-
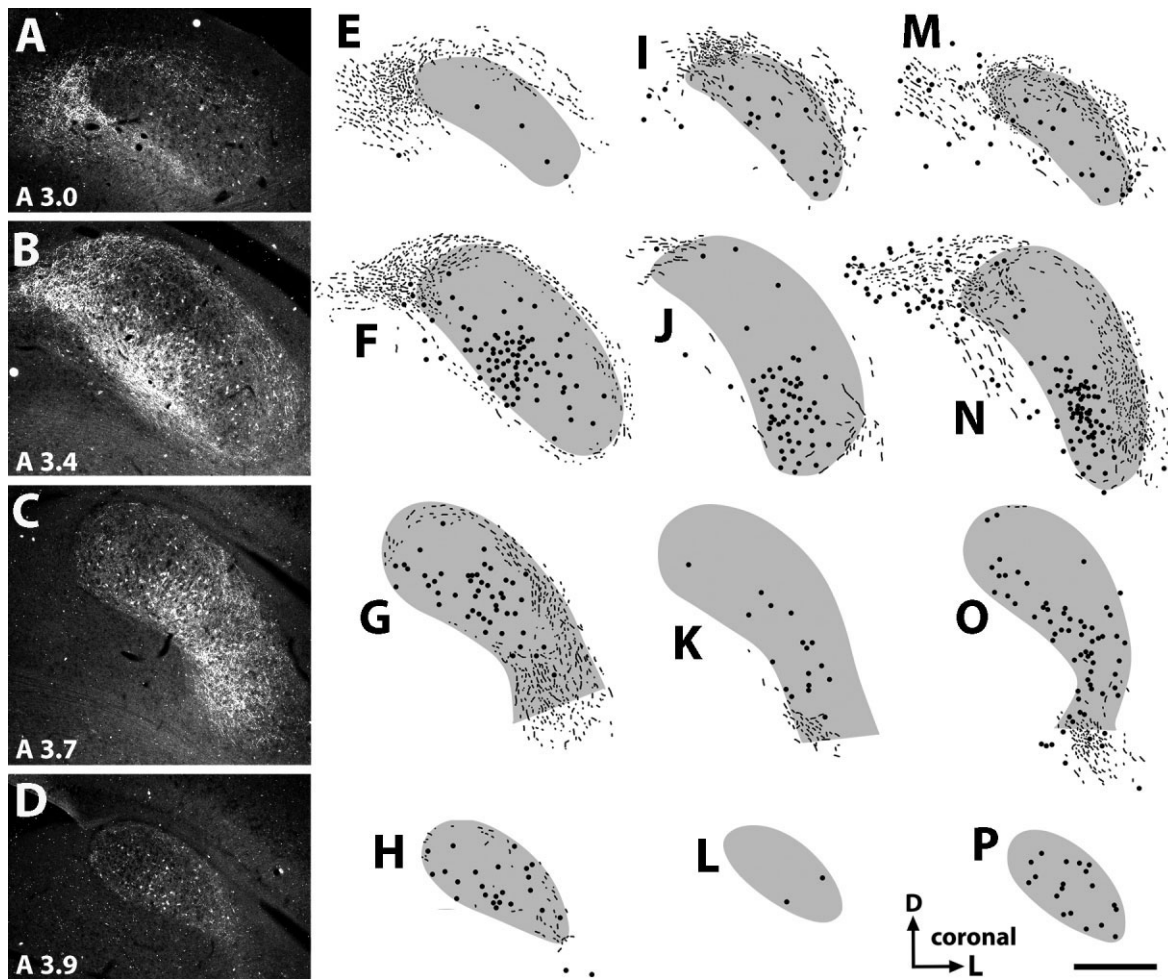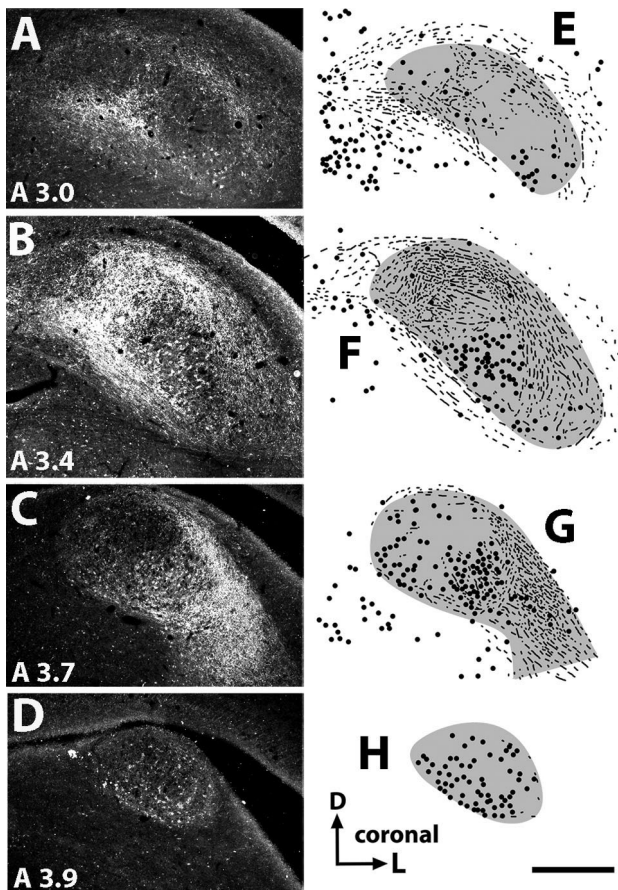
Figure 12. Low-magnification darkfield images and line drawings of anterograde and retrograde labeling in the contralateral MLd following injections of CTB into the NA-recipient zone of the MLd. **A–D:** Images of labeling following an injection into the caudal portion of the MLd (case 419). Numbers below each image indicate the approximate anterior-posterior stereotaxic levels. **E–H:** Line drawings of A–D, respectively. Solid black circles and lines indicate retrogradely labeled neurons and anterogradely labeled neuropil, respectively. **I–L:** Line drawings of labeled neurons and terminals following an injection into the ventral portion of the MLd (case 322). The approximate anterior-posterior levels of I–L are comparable to those in A–D. **M–P:** Line drawings of labeled neurons and terminals following an injection into the dorsal portion of the MLd (case 333). The approximate anterior-posterior levels of M–P are comparable to those in A–D. All three cases produced a similar distribution of labeled neurons and terminals in the contralateral MLd. A central region along the medial border of the nucleus, corresponding to the NL-recipient zone, contained a high density of labeled neurons. Anterogradely labeled terminals were mainly distributed along the periphery of the nucleus. Injection sites are illustrated in Figure 8. Scale bar = 500 μm in P (applies to A–P).

tain a comparable set of tonotopic representations with a wide frequency range (Boord and Rasmussen, 1963; Hotta, 1971; Rubel and Parks, 1975; Warchol and Dallos, 1990; Köppl, 2001). The current study further demonstrated that the separation of these two pathways has developed in hatchling chicks, consistent with the view that the general organization of the auditory system is stabilized in chicks after hatching (for review, see Rubel and Parks, 1988). In addition, we described the general topography of the projection from the NA upon the MLd, approximately consistent with the previous observation in pigeons (Leibler, 1975). Although the tonotopic organization of the MLd has not been mapped in chicks, this topog-

raphy is consistent with the tonotopic organization of the MLd in zebra finches (Woolley and Casseday, 2004), with the dorsal NA (high frequency) projecting to the ventral MLd (high frequency), and the ventral NA (low frequency) to the dorsal MLd (low frequency). The NA-recipient zone of the MLd may be further divided into several smaller subzones.

The discharging pattern of the neurons in the NA-recipient zone of the MLd varies in relationship to their location, with mainly "simple" neurons in the ventral portion and a high proportion of "complex" neurons in the dorsal portion (Scheich et al., 1977). In addition, different portions of the NA-recipient zone of the MLd terminate

Figure 13. Low-magnification darkfield images (**A–D**) and line drawings (**E–H**) of anterograde and retrograde labeling in the contralateral MLd following an injection of CTB into the NL-recipient zone of the MLd (case 319). The injection also involved the adjacent region of the NA-recipient zone, as illustrated in Figure 8. E–H are line drawings of A–D, respectively. Numbers below each image indicate the approximate anterior-posterior stereotaxic levels. Solid black circles and lines indicate retrogradely labeled neurons and anterogradely labeled neuropil, respectively. In the contralateral MLd, anterogradely labeled terminals were found extensively in the NA-recipient zone, especially in its dorsal portion. The NL-recipient zone contained densely labeled neurons but was lacking anterogradely labeled terminals. Scale bar = 500 μm in H (applies to A–H).

restrictively within several cytoarchitecturally distinct subdivisions of the auditory thalamus (Wang and Karten, unpublished observations). The small volume of the NL-recipient zone in chicks and our relatively large injection sites in the NL do not allow us to map the topography of the projection from the NL upon the MLd. In barn owls, this projection is organized in a topographical manner (Takahashi and Konishi, 1988a), and units in the NL-recipient zone of the MLd (also called ICCcore in barn owls) are arranged in a frequency-dependent order (Knudsen and Konishi, 1978; Wagner et al., 1987, 2002).

More importantly, we clarified the presence of a third separate ascending pathway from the caudodorsal brainstem upon the rostromedial MLd. This pathway was first differentiated by Conlee and Parks (1986) due to its distinct bilateral property. The current study further identified the major neuronal sources of this projection in the regions adjacent to the NM, NL, and NA at their caudal level, which is termed the RI in the current study, as well as from scattered neurons along the 8th nerve tract, and probably a very ventral portion of the NA. Although our data do not support a bilateral projection from the caudal NL upon the MLd, they do not exclude the possibility that the caudal NL sends a contralateral projection to the rostromedial MLd. At the midbrain level, the target of the bilateral projections constitutes a unique and cytoarchitectonically distinct portion of the auditory midbrain. They possess unique reciprocal commissural connections (the current study), maintain intensive 2-deoxyglucose staining, and display frequency selectivity with an oscillating discharge pattern after binaural cochlear removal (Heil and Scheich, 1986; Schwarz et al., 1993), features that are not common to neurons in other portions of the MLd. In addition, the rostromedial portion of the MLd in zebra finches shows a distinctive cytoarchitecture, although it is less pronounced in chicks (Karten, unpublished observations).

These unique features characterizing the neurons and their innervation in this pathway may provide the anatomic basis for a third, functionally unique channel. In barn owls, the first two channels code time and intensity information, respectively (for review, see Carr and Code, 2000). Bilateral properties of the third channel suggest that these neurons may be involved in interaural processing. In addition, Theurich et al. (1984) reported that the rostromedial MLd contains neurons sensitive to acoustic stimuli between 2 and 10 Hz, suggesting the involvement of this channel in processing acoustic information at very low frequencies. Warchol and Dallos (1989) reported that some neurons in the NA are sensitive to low frequency and infrasound between 10 and 50 Hz. Although the authors did not specify the location of these neurons, they did mention that non-auditory neurons were found "immediately ventral and medial" to low-frequency units. The authors assumed these non-auditory neurons were vestibular neurons. If this assumption is valid, the low-frequency neurons should distribute along the ventral and medial margins of the NA, where we found neurons with bilateral projections upon the MLd.

A pathway comparable to this third channel in chicks has not been identified in barn owls or pigeons. Neither retrograde nor anterograde tracing studies in barn owls showed evidence of a bilateral projection from the NM/NL/NA and/or their adjacent region to the MLd (Takahashi and Konishi, 1988a). In pigeons, a very small number of labeled neurons was found in the ipsilateral NL and NA following large injections into the MLd (Leibler, 1975). Following more restricted injections into the rostromedial
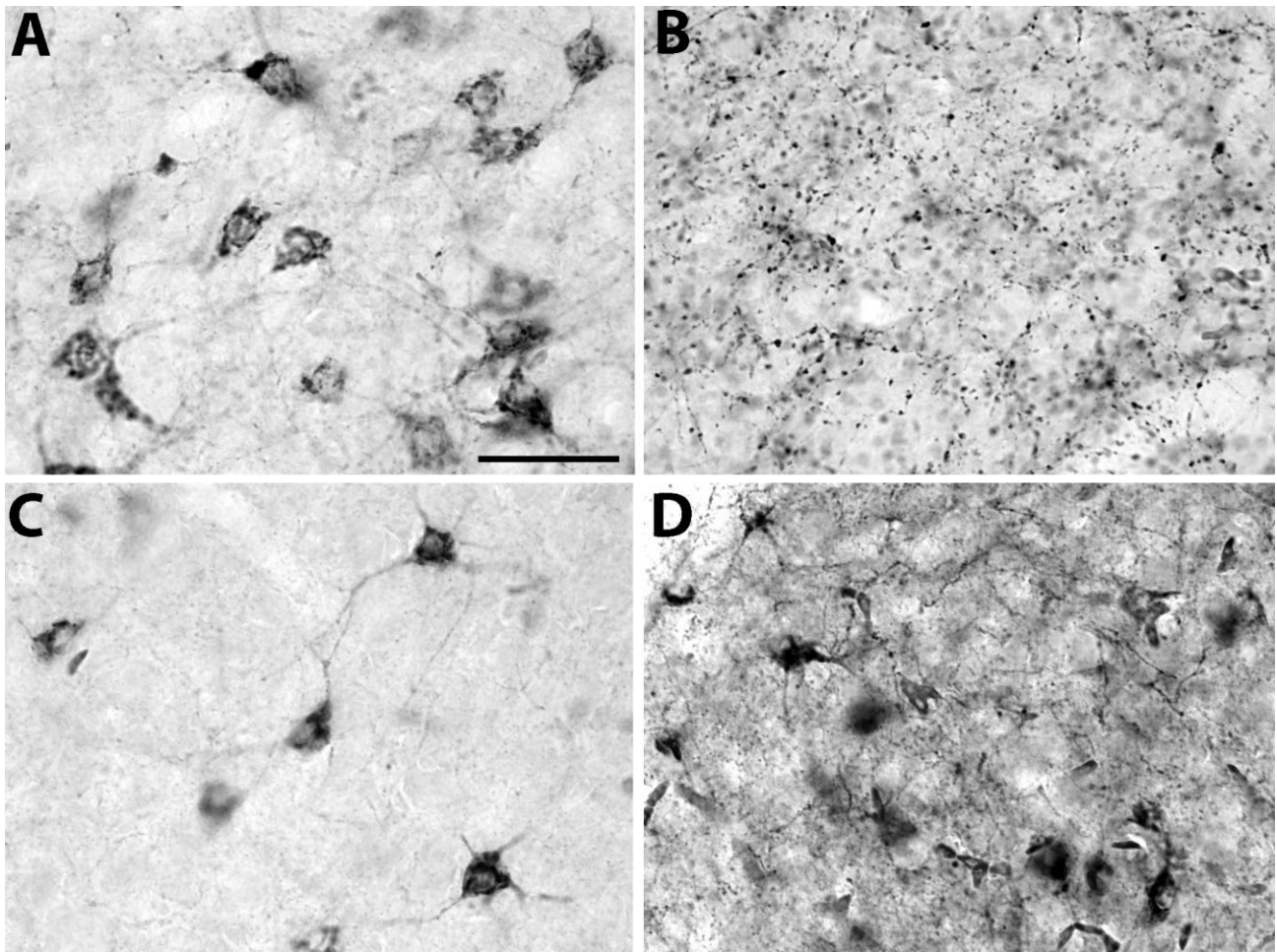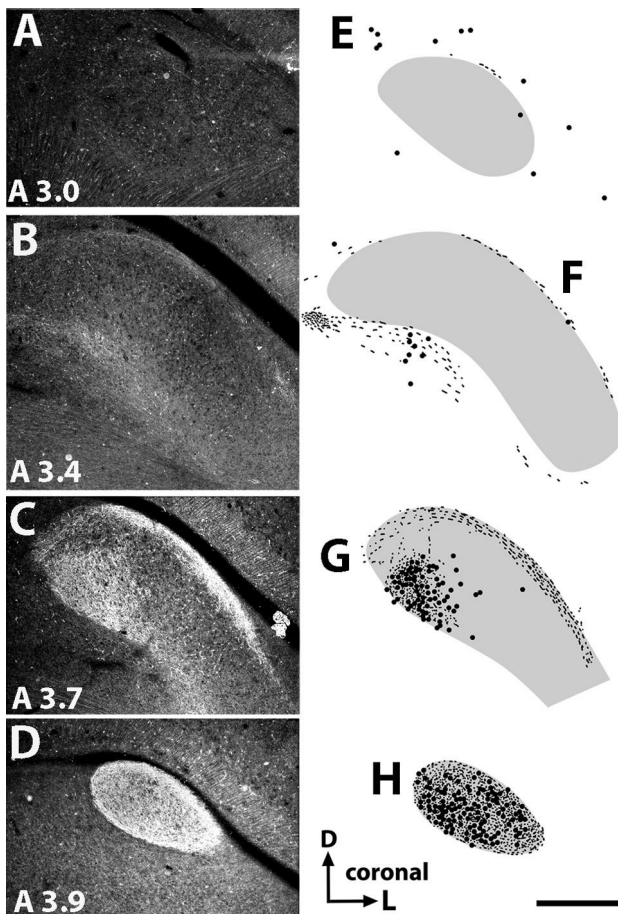
Figure 14. High-magnification brightfield images of the anterograde and retrograde labeling in the MLd following injections of CTB in the contralateral MLd. **A:** Retrogradely labeled neurons in the NL-recipient zone following the injection into the caudal portion of the NA-recipient zone (case 419). **B:** Anterogradely labeled terminals in the NA-recipient zone following the injection into the NL-recipient zone (case 319). **C:** Retrogradely labeled neurons in the NL-recipient zone in case 319. **D:** Retrogradely labeled neurons and anterogradely labeled terminals in the bilateral zone of the MLd following the injection into the same zone on the other side of the brain (case 418). In addition to darkly labeled cell bodies, a high density of small boutons and terminals formed a dark granular appearance of staining in this region, in contrast to the unstained, pale background in C. Scale bar = 50 μm in A (applies to a–D).

portion of the MLd, labeled neurons were detected surrounding the caudal NL and between the caudal NL and NA (Leibler, 1975; Wild, 1995). However, these neurons were reported only on the contralateral side. These interspecies variations raise interesting questions regarding species-specific animal behaviors in relationship to the organization of the auditory midbrain.

Two different views on nomenclature

Due to the immediately adjacent and partially overlapped location of the bilateral projecting neurons in the caudorostral brainstem with remaining neurons in the NM, NL, and NA, there are two different views on how to name the bilateral input to the avian auditory midbrain to facilitate further research in the system.

One view is that the bilateral projecting neurons in the caudodorsal brainstem should be treated as the very low frequency regions of the NL and NA. First, the distribution of the RI, one of the major origins of the bilateral projection to the MLd, overlaps with the termination and nerve tract of a fiber bundle of the 8th nerve arising from the inner ear. The exact origin of this fiber bundle was reported as the lagenar in pigeons (Boord and Rasmussen, 1963; Boord and Karten, 1974) and more recently described as the low-frequency region of the cochlea in chicks (Kaiser and Manley, 1996). Second, although the NA contains several physiologically and anatomically distinct cell types (Häusler et al., 1999; Soares et al., 2002; Köppl and Carr, 2003), only one tonotopic representation was recorded in the NA (Hotta, 1971; Warchol and Dallos, 1990; Köppl,

Figure 15. Low-magnification darkfield images (A–D) and line drawings (E–H) of anterograde and retrograde labeling in the contralateral MLd following the injection into the bilateral zone of the MLd (case 418). The retrograde and anterograde labeling was restricted to the bilateral zone of the contralateral MLd. Solid black circles and lines indicate retrogradely labeled neurons and anterogradely labeled neuropil, respectively. Numbers below each photo indicate the approximate anterior-posterior stereotaxic levels. The injection site is illustrated in Figure 8. Scale bar = 500 μm in H (applies to A–H).

2001). In barn owls, the same cell types are distributed along the tonotopic axis (Soares and Carr, 2001). An obvious disadvantage of grouping these neurons as parts of the NA and NL is increased ambiguity in the definition and description of the NM, NL, and NA, because a large portion of the bilateral projecting neurons are clearly located outside the traditional boundaries of these three nuclei.

An alternative view is that these bilateral projecting neurons should be considered as distinct cell groups in addition to the NM, NL, and NA. The major rationale underlying this view is the unique connectional features of these bilaterally projecting neurons. Primary cochlear nuclei NM and NA and secondary cochlear nucleus NL have been extensively studied both physiologically and anatomically. Two well-established definitions are that NL neurons do

not receive inputs from the periphery (Parks and Rubel, 1978) and that NM neurons do not project upon the midbrain (Boord, 1968; Leibler, 1975; Conlee and Parks, 1986; Takahashi and Konishi, 1988a). Direct inputs from the inner ear and outputs to the midbrain distinguish the neurons in the RI from NM and NL neurons. In addition, the bilateral property of the projection from neurons in the RI and the ventral NA to the MLd clearly indicates their distinct roles in processing auditory signals compared with the neurons in the NL and the major body of the NA. Furthermore, scattered neurons embedded in the 8th nerve tract clearly do not belong to the NM, NL, or NA. Because the bilaterally projecting neurons are innervated in a similar manner, it is reasonable to treat them as a whole structure with distinct functions from the NM, NL, and NA.

Commissural connections of the MLd

Equally importantly, the current study demonstrated that the three subdivisions of the MLd, identified on the basis of their differential afferent projections, also play distinct roles in the commissural connections of the MLd, which further supports the notion that these three subdivisions are functionally distinct. Two major components of the commissural connections of the MLd have been identified: a heavy projection from the NL-recipient zone upon the contralateral NA-recipient zone and a highly restricted reciprocal connection between the RI-recipient zones of two sides. The commissural projection from the NL-recipient zone to the NA-recipient zone has been previously identified in barn owls (Takahashi et al., 1989). However, this projection innervates the whole range of the NA-recipient zone in chicks but is restricted to the lateral portion of the owl NA-recipient zone. As this projection integrates time and intensity information and has been considered to contribute to the computation of the spatial location of auditory stimuli in barn owls, it would be interesting to study whether this is the case in chicks and, if so, why this projection expands in a species with less sensitivity to sound localization than barn owls.

Comparison of commissural connections of the MLd between chicks and pigeons is somewhat confusing. Studies in pigeons reported that the rostromedial MLds on two sides of the brain are reciprocally connected (Leibler, 1975; Wild, 1995), consistent with our observation in chicks. However, both authors reported that the rostromedial portion of the pigeon MLd is the major target of the contralateral NL. Reciprocal connections between the NL-recipient zones of the MLd are not found in chicks or barn owls. The functional significance of this second integration of binaural time information at the midbrain level in pigeons after the first convergence of acoustic information from the two ears within the NL remains unknown.
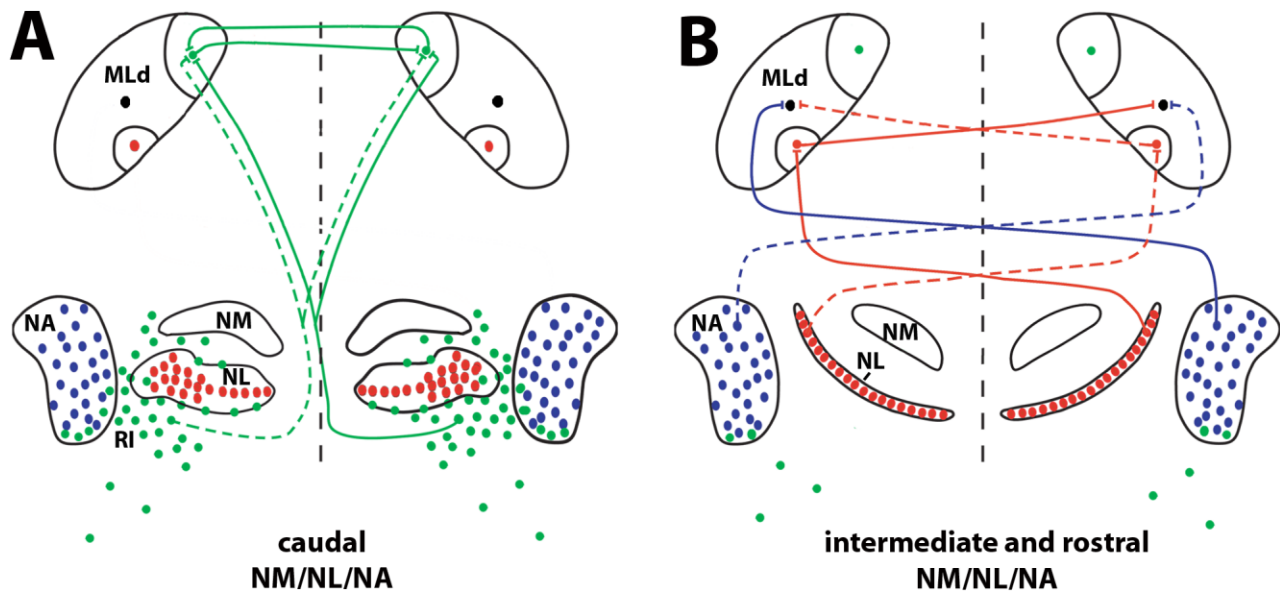
Figure 16. Schematic drawing of the afferent and commissural organization of the MLd. The dorsal auditory brainstem sends three separate pathways (green, red, and blue) upon three distinct subdivisions of the MLd. Filled circles and lines indicate neurons and connections in each pathway, respectively. Solid and dashed lines indicate connections issued from the right and left sides of the brainstem, respectively. For the purpose of clarity, the red and blue pathways in A are not illustrated; the organization of these connections is the same as demonstrated in B. The green pathways are illustrated in A as the majority of the neurons in the green channel at the brainstem level are located in the caudal portion. The NA-recipient zone of the MLd, shown as black cells, receives information from both red and blue channels. However, whether individual neurons in the NA-recipient zone receive direct bilateral inputs requires further investigation. The ipsilateral projections from the NL and NA upon the MLd, the projection from the NA upon the NL-recipient zone of the MLd, and the connections between the NA-recipient zones of two sides, are very sparse, and not included in the drawing. Abbreviations: NL, nucleus laminaris; NA, nucleus angularis; NM, nucleus magnocellularis; RI, regio intermedius; MLd, nucleus mesencephalicus lateralis pars dorsalis.

Comparison with mammals

The central nucleus of the inferior colliculus (ICC) in mammals is the major recipient of the ascending projections from the auditory brainstem including the cochlear nuclei, the superior olive complex, and the lateral lemniscus nuclei (Oliver and Huerta, 1992), comparable to the information convergence in the avian MLd. A recent tracing study in gerbils divided the ICC into two subdivisions, one receiving inputs from both the cochlear nuclei and the superior olive, and the other from only the cochlear nuclei (Cant and Benson, 2006). The avian NL is thought to be homologous or analogous to the medial superior olivary nucleus of mammals (Ramón y Cajal, 1909–1911; Burger and Rubel, 2008), although the extent of this postulated homology remains controversial (Grothe et al., 2004). Neurons in the NA display a similar range of response types to sound stimuli as in the mammalian cochlear nuclei (Köppl and Carr, 2003). Thus, two ICC subdivisions identified in gerbils may be generally compared to the NL- and NA-recipient zones of the avian MLd, respectively. Birds and mammals may differ in the organization of the commissural connections of the auditory midbrain. In mammals, this connection is reciprocal and is topographically organized throughout the nucleus (Saldaña and Merchán, 1992; Malmierca et al., 1995, 2005), in contrast to the region-region specificity in birds.

CONCLUSIONS

Multiple, parallel auditory brainstem pathways converge in the avian MLd and the mammalian ICC. As a consequence, the auditory midbrain has been suggested to be a major site of neural integration and to be involved in a number of auditory tasks, including sound localization and coding of complex acoustic signals such as birdsong and vocalization. One of the requirements necessary for performing these auditory tasks is the ability to organize and integrate various properties of acoustic signals (time, intensity, and frequency) in a highly specific pattern. The heterogeneous organization of the auditory midbrain, with differential afferents to several distinct subdivisions and specialized interactions among these subdivisions, may provide the anatomical basis for this capability. Further studies on the detailed organization of the neuronal network in each subdivision will be essential to understand the cellular substrates underlying the function of the auditory midbrain.

ACKNOWLEDGMENTS

LITERATURE CITED

Adolphs R. 1993. Acetylcholinesterase staining differentiates functionally distinct auditory pathways in the barn owl. J Comp Neurol 329:365–377.

Boord RL. 1968. Ascending projections of the primary cochlear nuclei and nucleus laminaris in the pigeon. J Comp Neurol 133:523–541.

Boord RL, Karten HJ. 1974. The distribution of primary lagenar fibers within the vestibular nuclear complex of the pigeon. Brain Behav Evol 10:228–235.

Boord RL, Rasmussen GL. 1963. Projection of the cochlear and lagenar nerves on the cochlear nuclei of the pigeon. J Comp Neurol 120:463–475.

Burger RM, Rubel EW. 2008. Encoding of interaural timing for binaural hearing. In: Dallos P, Oertel D, editors. The senses: a comprehensive reference. San Diego: Academic Press. p 613–630.

Cant NB, Benson CG. 2006. Organization of the inferior colliculus of the gerbil (*Meriones unguiculatus*): differences in distribution of projections from the cochlear nuclei and the superior olivary complex. J Comp Neurol 495:511–528.

Carr CE, Code RA. 2000. The central auditory system of reptiles and birds. In: Dooling RJ, Fay RR, Popper AN, editors. Comparative hearing: birds and reptiles. New York: Springer-Verlag. p 197–248.

Conlee JW, Parks TN. 1986. Origin of ascending auditory projections to the nucleus mesencephalicus lateralis pars dorsalis in the chicken. Brain Res 367:96–113.

Grothe B, Carr CE, Casseday JH, Fritzsch B, Köppl C. 2004. The evolution of central pathways and their neural processing patterns. In: Manley GA, Popper AN, Fay RR, editors. Evolution of the vertebrate auditory system. New York: Springer-Verlag. p 289–359.

Häusler UH, Sullivan WE, Soares D, Carr CE. 1999. A morphological study of the cochlear nuclei of the pigeon (*Columba livia*). Brain Behav Evol 54:290–302.

Heil P, Scheich H. 1986. Effects of unilateral and bilateral cochlear removal on 2-deoxyglucose patterns in the chick auditory system. J Comp Neurol 252:279–301.

Holmes G. 1903. On the comparative anatomy of the nervus acusticus. Trans R Irish Acad B 32:101–144.

Hotta T. 1971. Unit responses from the nucleus angularis in the pigeon's medulla. Comp Biochem Physiol A 40:415–424.

Iñiguez C, Gayoso MJ, Carreres J. 1985. A versatile and simple method for staining nervous tissue using Giemsa dye. J Neurosci Methods 13:77–86.

Kaiser A, Manley GA. 1996. Brainstem connections of the macula lagenae in the chicken. J Comp Neurol 374:108–117.

Karten HJ. 1967. The organization of the ascending auditory pathway in the pigeon (*Columba livia*). 1. Diencephalic projections of the inferior colliculus (nucleus mesencephali lateralis, pars dorsalis). Brain Res 6:409–427.

Karten HJ. 1968. The ascending auditory pathway in the pigeon (*Columba livia*). II. Telencephalic projections of the nucleus ovoidalis thalami. Brain Res 11:134–153.

Klump GM. 2000. Sound localization in birds. In: Dooling RJ, Fay RR, Popper AN, editors. Comparative hearing: birds and reptiles. New York: Springer-Verlag. p 249–307.

Knudsen EI. 1987. Neural derivation of sound source location in the barn owl. An example of a computational map. Ann N Y Acad Sci 510:33–38.

Knudsen EI, Konishi M. 1978. Space and frequency are represented separately in auditory midbrain of the owl. J Neurophysiol 41:870–884.

Konishi M, Sullivan WE, Takahashi T. 1985. The owl's cochlear nuclei process different sound localization cues. J Acoust Soc Am 78:360–364.

Köppl C. 2001. Tonotopic projections of the auditory nerve to the cochlear nucleus angularis in the barn owl. J Assoc Res Otolaryngol 2:41–53.

Köppl C, Carr CE. 2003. Computational diversity in the cochlear nucleus angularis of the barn owl. J Neurophysiol 89:2313–2329.

Kuenzel WJ, Masson M. 1988. A stereotaxic atlas of the brain of the chick (*Gallus domesticus*). Baltimore, MD: Johns Hopkins University Press.

Leibler LM. 1975. Monaural and binaural pathways in the ascending auditory system of the pigeon. Ph.D. Thesis, Massachusetts Institute of Technology, Cambridge, MA.

Malmierca MS, Rees A, Le Beau FE, Bjaalie JG. 1995. Laminar organization of frequency-defined local axons within and between the inferior colliculi of the guinea pig. J Comp Neurol 357:124–144.

Malmierca MS, Hernandez O, Rees A. 2005. Intercollicular commissural projections modulate neuronal responses in the inferior colliculus. Eur J Neurosci 21:2701–2710.

Oliver DL, Huerta MF. 1992. Inferior and superior colliculi. In: Webster DB, Popper AN, Fay RR, editors. The mammalian auditory pathway: neuroanatomy. New York: Springer-Verlag. p 168–221.

Parks TN, Rubel EW. 1978. Organization and development of the brain stem auditory nuclei of the chicken: primary afferent projections. J Comp Neurol 180:439–448.

Puelles L, Robles C, Martinez-de-la-Torre M, Martinez S. 1994. New subdivision schema for the avian torus semicircularis: neurochemical maps in the chick. J Comp Neurol 340:98–125.

Ramón y Cajal S. 1909-1911. Histologie du système nerveux de l'homme et des vertèbrès. Translated by L. Azoulay. Paris: Maloine.

Rubel EW, Parks TN. 1975. Organization and development of brain stem auditory nuclei of the chicken: tonotopic organization of n. magnocellularis and n. laminaris. J Comp Neurol 164:411–433.

Rubel EW, Parks TN. 1988. Organization and development of the avian brain-stem auditory system. In: Edelman GM, Gall WE, Cowans WM, editors. Auditory function: neurobiological bases of hearing. New York: John Wiley & Sons, Inc. p 3–92.

Saldaña E, Merchán MA. 1992. Intrinsic and commissural connections of the rat inferior colliculus. J Comp Neurol 319:417–437.

Scheich H, Langner G, Koch R. 1977. Coding of narrow-band and wide-band vocalizations in the auditory midbrain nucleus (MLD) of the guinea fowl (*Numida meleagris*). J Comp Physiol 117:245–265.

Schwarz DW, Dezso A, Neufeld PR. 1993. Frequency selectivity of central auditory neurons without inner ear. Acta Otolaryngol 113:266–270.

Soares D, Carr CE. 2001. The cytoarchitecture of the nucleus angularis of the barn owl (*Tyto alba*). J Comp Neurol 429:192–205.

Soares D, Chitwood RA, Hyson RL, Carr CE. 2002. Intrinsic neuronal properties of the chick nucleus angularis. J Neurophysiol 88:152–162.

Sullivan WE, Konishi M. 1984. Segregation of stimulus phase and intensity coding in the cochlear nucleus of the barn owl. J Neurosci 4:1787–1799.

Takahashi T, Konishi M. 1986. Selectivity for interaural time difference in the owl's midbrain. J Neurosci 6:3413–3422.

Takahashi T, Konishi M. 1988a. The projections of the cochlear nuclei and nucleus laminaris to the inferior colliculus of the barn owl. J Comp Neurol 274:190–211.

Takahashi T, Konishi M. 1988b. Projections of nucleus angularis and nucleus laminaris to the laterallemniscal nuclear complex of the barn owl. J Comp Neurol 274:212–238.

Takahashi T, Moiseff A, Konishi M. 1984. Time and intensity cues are processed independently in the auditory system of the owl. J Neurosci 4:1781–1786.

Takahashi T, Carr CE, Brecha N, Konishi M. 1987. Calcium binding protein-like immunoreactivity labels the terminal field of nucleus laminaris of the barn owl. J Neurosci 7:1843–1856.

Takahashi T, Wagner H, Konishi M. 1989. Role of commissural projections in the representation of bilateral space in the barn owl's inferior colliculus. J Comp Neurol 281:545–554.

Theurich M, Langner G, Scheich H. 1984. Infrasound responses in the midbrain of the guinea fowl. Neurosci Lett 49:81–86.

Wagner H, Takahashi T, Konishi M. 1987. Representation of interaural time difference in the central nucleus of the barn owl's inferior colliculus. J Neurosci 7:3105–3116.

Wagner H, Mazer JA, von Campenhausen M. 2002. Response properties of neurons in the core of the central nucleus of the inferior colliculus of the barn owl. Eur J Neurosci 15:1343–1352.

Wagner H, Güntürkün O, Nieder B. 2003. Anatomical markers for the subdivisions of the barn owl's inferior-collicular complex and adjacent peri- and subventricular structures. J Comp Neurol 465:145–159.

Warchol ME, Dallos P. 1989. Neural response to very low-frequency sound in the avian cochlear nucleus. J Comp Physiol A 166:83–95.

Warchol ME, Dallos P. 1990. Neural coding in the chick cochlear nucleus. J Comp Physiol A 166:721–734.

Wild JM. 1995. Convergence of somatosensory and auditory projections in the avian torus semicircularis, including the central auditory nucleus. J Comp Neurol 358:465–486.

Woolley SM, Casseday JH. 2004. Response properties of single neurons in the zebra finch auditory midbrain: response patterns, frequency coding, intensity coding, and spike latencies. J Neurophysiol 91:136–151.

Woolley SM, Casseday JH. 2005. Processing of modulated sounds in the zebra finch auditory midbrain: responses to noise, frequency sweeps, and sinusoidal amplitude modulations. J Neurophysiol 94:1143–1157.

Woolley SM, Gill PR, Theunissen FE. 2006. Stimulus-dependent auditory tuning results in synchronous population coding of vocalizations in the songbird midbrain. J Neurosci 26:2499–2512.